

AN ABSTRACT OF THE THESIS OF

Jonathan M. Lebsack for the degree of Master of Science in Chemical Engineering presented on March 20, 2012.

Title: Efficiency of a Direct Contact Condenser in the Presence of the Noncondensable Gas Air Compared to a Tube and Shell Condenser

Abstract approved:

David E. Hackleman

Steam distillation is the traditional method used for the extraction of peppermint oil. This process is able to remove approximately 20% of the oils from the leaves of the plant. It is a very costly and un-sustainable process due to the release of carbon emissions. Solvent free microwave extraction promises yields of up to 65% of the “available” oils from the peppermint at 3% less cost (Velasco 2007). It can also reduce carbon emissions because it will be using electricity as a power source instead of fossil fuels, however not all electric companies use renewable energies. In 2009 a SFME pilot plant was assembled in North Carolina to test the efficiency of the microwave process on a larger than lab scale. Results from the experiments showed that the tube and shell condenser was unable to effectively condense the mint oil. The problem was determined to be the addition of air to the mixture due to the open ends of the microwave. However it was discovered that the spray scrubber after the condenser was able to collect a visible amount of oil. This inspired the design of a

direct contact condenser (Pommerenck 2012). The direct contact condenser they designed, built, and tested showed vast improvements in steam capturing efficiency when compared to a tube and shell condenser. However due to the materials used for its construction it could not sustain operating temperatures seen in the microwave pilot plant. Using their design a new direct contact condenser was built using materials that would be able to withstand heavy temperatures. The condenser was constructed out of aluminum and contained stainless steel spray nozzles, both for their non-corrosive properties. Tests were conducted using 8 and 16 nozzles and tested over a range of 20-100% steam by mass. Additional tests were completed using the full 24 nozzles but due to the location of some of the nozzles coolant was lost as an aerosol with no way to quantify the loss. Comparing the data to research completed by Pommerenck et al. on efficiency of a tube and shell condenser used for the mint distillation process found that with increasing amounts of air there is a greater loss of heat transfer. This is believed to be the effects of a boundary layer of the noncondensable fluid, air, which forms along the tube and resists condensation from forming (Seunguim 2006). Pommerenck's tube and shell condenser used a coolant flow rate of 24 L/min while the flow rates tested in this research were 18 L/min and 36 L/min. The direct contact condenser showed a considerable increase in performance even with the smaller flow rate compared to the tube and shell unit, indicating removal of the boundary layer. The efficiency tends to follow the maximum theoretical efficiency while the tube and shell condenser lowers in efficiency. The overall goal of this project is to determine the feasibility of the use of a direct contact condenser for implementation in the solvent free microwave extraction of peppermint oil when air is present.

©Copyright by Jonathan M. Lebsack
March 20, 2012
All Rights Reserved

Efficiency of a Direct Contact Condenser in the Presence of the Noncondensable Gas
Air Compared to a Tube and Shell Condenser

by
Jonathan M. Lebsack

A THESIS

Submitted to

Oregon State University

In partial fulfillment of
the requirements for the
degree of

Master of Science

Presented March 20, 2012
Commencement June 2012

Master of Science thesis of Jonathan M. Lebsack presented on March 20, 2012

APPROVED:

Major Professor, representing Chemical Engineering

Head of the School of Chemical, Biological and Environmental Engineering

Dean of the Graduate School

I understand that my thesis will become part of the permanent collection of Oregon State University libraries. My signature below authorizes release of my thesis to any reader upon request.

Jonathan M. Lebsack, Author

ACKNOWLEDGEMENTS

I would like to thank Dr. Hackleman for giving me the opportunity and the time of out his busy life to work on this project with him. In addition I would like to thank the Mint Industry Research Council for the opportunity to come discuss the research we have been working on and for funding a portion of the project. I also thank the OSU Foundation for its funding of my research stipend. Finally, I would like to thank my family who motivated me by telling me there was no way I could finish writing my thesis in one term.

I would also like to thank John Reerslev and Richard Mattix. John for allowing me to go to his farm and take mint samples; as well as give me a tour of his distillation facility. Richard for allowing me to store the mint samples out in the freezer at Hyslop Farms.

I would also like to give a special thanks to the ChE 416 team; Justin Pommerenck, Yousef Alanazi, Richard Vachkov, and Troy Gzik. The work their team did on the project set the foundation and path for my own research.

TABLE OF CONTENTS

	<u>Page</u>
1. Introduction.....	1
2. Literature Review.....	2
2.1 Essential Oils.....	2
2.2 Peppermint Oil Composition.....	2
2.3 Peppermint Oil Secretion.....	5
2.4 Steam Distillation.....	7
2.5 Solvent Free Microwave Extraction.....	10
3. Materials.....	15
3.1 Steam Generation Hood.....	15
3.2 Direct Contact Condenser.....	15
3.3 Nozzles.....	18
4. Methods.....	20
4.1 Experimental Design.....	20
4.2 Material Balance.....	22
4.3 Maximum Efficiency.....	26
5. Results.....	27
5.1 Temperature Profiles.....	27
5.2 Efficiency Results.....	28
5.3 Condenser Capacity.....	29
5.4 Scale Up.....	30
5.5 Velocity of Gas.....	31
5.6 Separation.....	32
6. Conclusion.....	33
7. Future Work.....	36
7.1 Direct Contact Condenser Field Test.....	36
7.2 Direct Solar Generation.....	36
7.3 Coolant Water Recycle.....	38

TABLE OF CONTENTS (Continued)

	<u>Page</u>
8. Bibliography.....	41
9. Appendices.....	43
Appendix A- Specification of Condenser Shell.....	44
Appendix B- Coolant Pump Specifications.....	46
Appendix C- Nozzle Specifications.....	48

LIST OF FIGURES

<u>Figure</u>	<u>Page</u>
2.31 Microscopy Post-Secretory Stage of the Peltate Glandular.....	5
2.32 Illustration of the Peltate Glandular.....	5
2.33 The Methyl Erythritol Phosphate Pathway.....	6
2.34 Oil Composition vs. Age of Leaf.....	7
2.41 Saturation Pressure of the Mixture based on Raoult's Law.....	8
2.42 Boiling Temperature of the Mixture based on Raoult's Law.....	8
2.43 Steam Distillation Unit with a Portable Tub.....	8
2.44 Carbon Emissions based on Farm Activities.....	10
2.51 SEM Peppermint leaf prior to Microwave Extraction.....	11
2.52 SEM Peppermint leaf post Microwave Extraction.....	11
2.53 Flow Sheet Diagram from North Carolina Experiments.....	12
2.54 Spray Scrubber for Microwave Pilot Plant.....	13
2.55 Inside of Spray Scrubber for Microwave Pilot Plant.....	13
 3.11 Steam Hood with Steam Manifold.....	 15
3.21 Design of the Direct Contact Condenser.....	16
3.22 Aluminum Direct Contact Condenser Experimental Set-Up.....	17
3.31 Number of Nozzles based on Coolant Temperature.....	19
 4.11 Aspen HYSYS Results for Mixing Temperature Based on % Steam by Mass...	 20
4.12 Flow Diagram for the Experimental Set-Up.....	21
4.21 Saturation Vapor Density of Air from 0°C to 100°C.....	22
4.22 Aspen HYSYS Results for Mixture Density Based on Mixing Temperature.....	24
4.23 Flow Block Diagram for Direct Contact Condenser.....	25

LIST OF FIGURES (Continued)

<u>Figure</u>	<u>Page</u>
4.31 Maximum Theoretical Efficiency with 115°F Exhaust.....	26
5.11 Coolant and Exhaust Temperatures for 16 Nozzles 85°C Test.....	27
5.12 Coolant and Exhaust Temperatures for 8 Nozzles 82°C Test.....	28
5.21 Measured Efficiencies for 8 and 16 Nozzles.....	29
5.31 Steam Recovery and Condenser Capacity for 16 Nozzle Tests.....	30
5.41 Scale Up-Number of Nozzles.....	31
5.51 Gas Velocity based on Mixing Temperature.....	32
6.11 Efficiency of Direct Contact Condenser compare to Tube and Shell.....	34
7.21 Direct Solar Irradiance over Junction City Oregon, August 1 st	36
7.22 Flow Diagram for Superheated Direct Solar Generation.....	37
7.31 Proposed Recycle Coolant Water Flow Diagram with Storage Tank.....	39
7.32 Current Coolant Water Flow Diagram.....	40
7.33 Proposed Recycle Coolant Water Flow Diagram with Chiller.....	40

LIST OF TABLES

<u>Table</u>	<u>Page</u>
2.21 Average Peppermint Oil Composition at Harvest.....	3
2.51 Experimental Condition for North Carolina Tests.....	13

LIST OF APPENDIX FIGURES

<u>Appendix</u>	<u>Page</u>
A. Condenser Shell Specifications.....	44
A.1 Side View.....	44
A.2 Platform.....	45
A.3 Top View.....	45
B. Sprayer Pump Specifications.....	46
B.1 Image of Pump.....	47
C. Nozzle Specifications.....	48
C.1 Lechler Axial Full Cone Nozzle Flow Rates.....	48

Efficiency of a Direct Contact Condenser in the Presence of the Noncondensable Gas Air Compared to a Tube and Shell Condenser

1. Introduction

Peppermint farming has traditionally been a major crop in the northwest. In 2010 California, Idaho, Oregon, and Washington grew a combined total of 56,700 acres of peppermint (Jenkins 2012). To this day farmers are still using the steam distillation method to extract peppermint oil from the plant material. The oil is then sold through distributors and specialty oil formulators such as A.M Todd and I.P. Callison to major brand companies such as Wrigley and Proctor and Gamble, to be used in cosmetics and food products.

Steam distillation is a very energy intensive process, particularly the generation of steam. The rising cost of natural gas and diesel has inspired research in to possible ways to improve efficiency and yield. Another issue that is just emerging is the need to reduce carbon emissions. Companies that purchase mint oil want to be able to market their products as sustainable and low emission. Due to a recent spike in diesel prices many farmers have been converting their boilers to natural gas. Natural gas is a much cleaner burning fuel and the conversion has only a 1-4 year payback. However, it is not clear if natural gas will remain at such a low price. The purpose of this research was to explore more sustainable options for the extraction process. Rocky Lundy, Executive Director of the Mint Industry Research Council, reported that 44% of carbon emissions from the entire process come from steam distillation (Gregory 2012). Dr. Hackleman has proposed a continuous microwave extraction process which promises a greater efficiency and oil yield utilizing the more stable energy price of electricity. However the open ends of the microwave allow air to enter the mixture. The air insulates the steam and traps it as humidity resulting in a loss of product.

2. Literature Review

2.1 Essential Oils

Traditional edible foods are no longer the only key plants in agricultural trade. Now plants that have secondary metabolites with aromatic and therapeutic properties are also considered valuable (Sangwan 2001). These aromatic volatile oils with distinct aromas produced from plants are known as essential oils. Essential oils have been used since before the recorded history of mankind and future trade in this area is expected to expand at a tremendous rate (Sangwan 2001).

Peppermint oil is an essential oil that is found in the leaves of the peppermint plant (*Mentha Piperita*). Peppermint oil is only one of many essential oils and is a hybrid of watermint and spearmint; two mints with very similar oil compositions (Craig 2004). Some other common essential oils include rose, oregano, sandalwood, and pine oils.

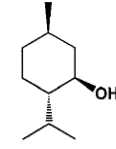
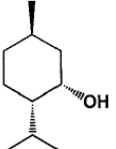
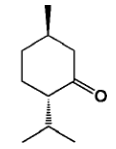
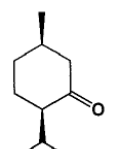
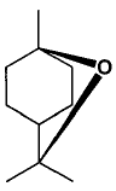
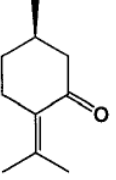
First described in 1696 the herb peppermint soon became very popular in England and the United States. The United States currently produces about 75% of the world's fresh supply (Siegel-Maier 1998). Farmers in the United States have been growing these crops for hundreds of years for use in everything from cosmetics to chewing gum and tea to cigarettes. Peppermint oil is also shown to have a variety of health benefits for users plagued with ailments such as headaches, congestion, and irritable bowel syndrome (Alam 2011).

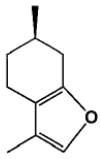
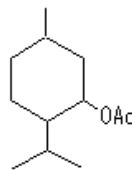
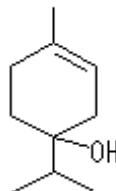
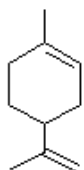
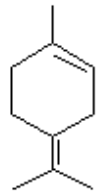
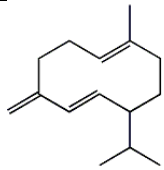
2.2 Peppermint Oil Composition

Monoterpenes comprise the major components of the essential oils of the mint family (Lawrence, 1981). Farmers and their customers are very concerned that the mint they produce retains the same flavor as it has since they were young. For this reason the same type of peppermint is planted because they know it will yield approximately the same composition of oil. However developmental and environmental factors are known to influence the yield and composition of peppermint oil so it will be impossible to recreate the exact composition from year to year (Burbott and Loomis,

1967). The average composition of monoterpenes and other compounds found in peppermint oil at the time of harvest can be found in Table 2.21.

Table 2.21- Average composition of major monoterpenes found in peppermint leaves at harvest (Velasco 2007).

	Compound	Chemical Structure	Percentage
Monoterpenes	(-)-Menthol		47% - 55%
	(+)-Neomenthol		1% - 3%
	(-)-Menthone		6% - 32%
	(+)-Isomenthone		1% - 3%
	1,8-Cineole		3% - 14%
	(+)-Pulegone		1% - 4%

	(+)-Menthofuran		1% - 8%
	Esters (Menthyl Acetate)		3% - 29%
	4-Terpeniol		1% - 5%
Monoterpene Olefins	Limonene		1 % - 6%
	Terpinolene		0.1% - 0.2%
Sesquiterpene	Germacrene-D		0.5% - 4.5 %

2.3 Peppermint Oil Secretion

Monoterpene biosynthesis and accumulation in peppermint is specifically localized to the glandular trichomes found in the leaf of the peppermint plant (Gershenzon et al. 1989). After secretion the oil is stored in a large cell known as the sub-cuticular oil storage cavity. “These glands arise from epidermal protuberances and produce a peltate trichome with one basal cell, a stalk cell, and a cytoplasmically dense apical cell. The apical cell then divides to produce a peltate trichome with one basal cell, one stalk cell, and eight glandular secretory cells (Turner, G. 2000).” Figure 2.31 is an image and shows the sub-cuticular oil storage space (SCS) above the glandular disc cells (GD); which are anchored to the leaf via the stalk cell (SC) and basal cell (BC). Figure 2.32 is an illustration of Figure 2.31 the only difference is the glandular disc cells are shown as secretory cells.

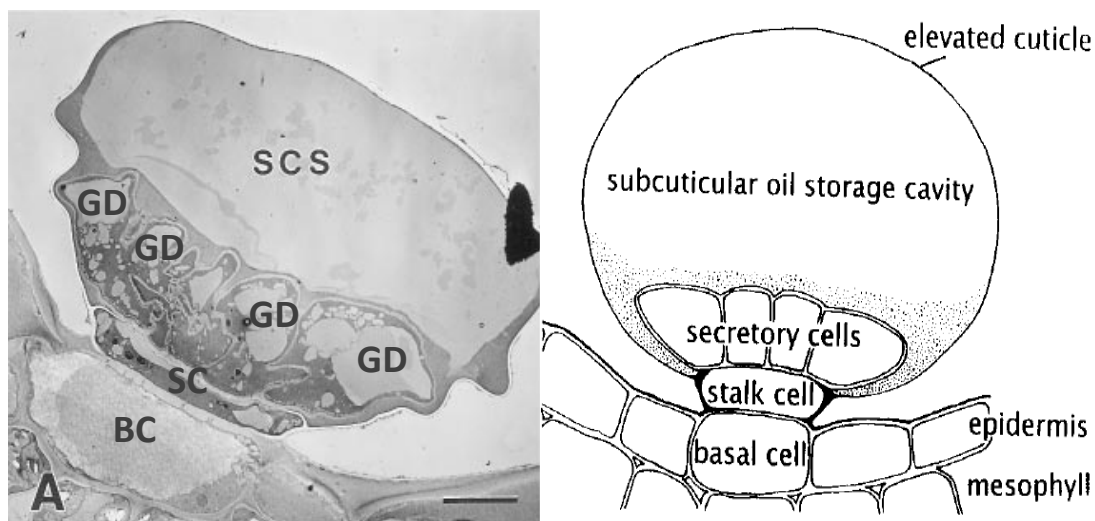


Figure 2.31 & 2.32- (Left) A chemically fixed post-secretory stage of the peltate glandular. The bar is 10 μm . (Right) An illustrated version of the same shot; the glandular disc cells are also known as the secretory cells because this is where the oil is secreted (Turner 2000, Turner 2000).

All of the monotrene derivatives found in peppermint oil are produced through the methyl erythritol phosphate pathway (MEP). The reaction pathway and enzyme are described in Figure 2.33 and the subsequent text.

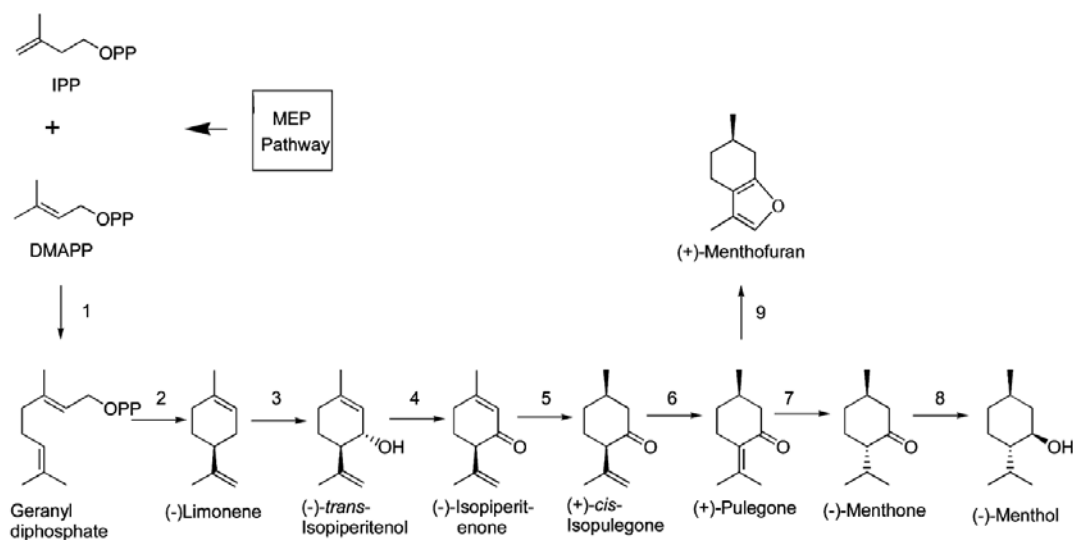


Figure 2.33- The methyl erythritol phosphate (MEP) pathway as described by (Wildung and Croteau 2005).

Menthol, both (-)-menthol and (+)-neomenthol, are the final products of eight step reaction pathway that begins with isopentenyl diphosphate and dimethylallyl diphosphate. The nine reactions in the MEP are catalyzed by the following enzymes: “(1) geranyl diphosphate synthase (GPPS), (2) (-)-(4S)-limonene synthase, (3) cytochrome P450 (-)-limonene-3-hydroxylase, (4) (-)-trans-isopiperitenol dehydrogenase, (5) (-)-isopiperitenone reductase, (6) (+)-cis-isopulegone isomerase, (7) (+)-pulegone reductase (PR), (8) (-)-menthone reductase (MR), and (9) cytochrome P450 (+)-menthofuran synthase (MFS) (Wildung and Croteau 2005).”

Monoterpene biosynthesis in peppermint glandular trichomes is restricted to leaves 12 to 20 days of age. While the final enzyme in the conversion to (-)-menthone is centered at 21 days (McConkey 2000). Leafs sampled over a period of 55 days were isolated via steam distillation-pentance extraction. The resulting extract was then run through gas chromatography; Figure 2.34 shows how the composition of oil changes over the lifetime of a leaf. Monoterpenes are considered volatile oils and most farmers are concerned with losses to the atmosphere. However, over a 6-month period, the typical growing period of the leaf, <5% of monoterpenes would be released to the atmosphere (Gershenzon 2000).

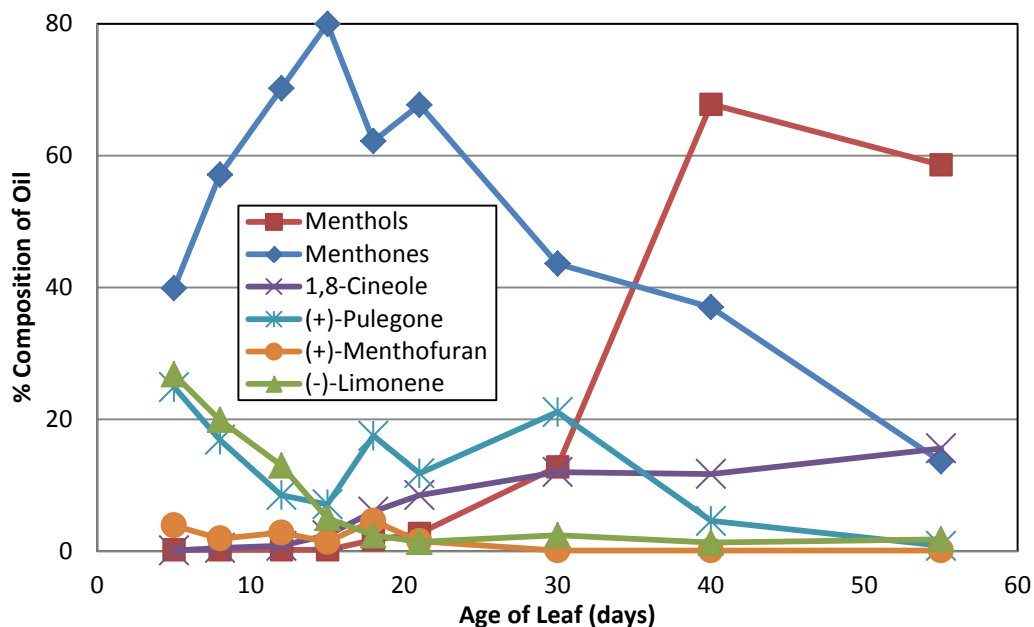


Figure 2.34- The changing oil composition from peppermint leaves as a function of age of leaf (Gershenzon 2000). Menthols include (-)-Menthol and (+)-Neomenthol, menthones include (-)-Menthone and (+)-Isomenthone.

2.4 Steam Distillation

Steam distillation is the most commonly used method for extraction of mint oil from peppermint plants. It uses steam to break apart the glandules and transport the peppermint oil out of the mint. The two main components of mint oil are menthone and menthol, which have boiling points of 207°C and 212°C, respectively (Sandborn 1929, C.R.C. 1971). Due to their large mole fractions the boiling point of peppermint will be somewhere within this region. So how can the mint be vaporized at such low temperatures?

Raoult's Law explains how the steam is able to remove the mint oil without it reaching its boiling temperature. Figures 2.41 and 2.42 show the relationship for vapor pressure and boiling temperature based on molar fraction of peppermint oil.

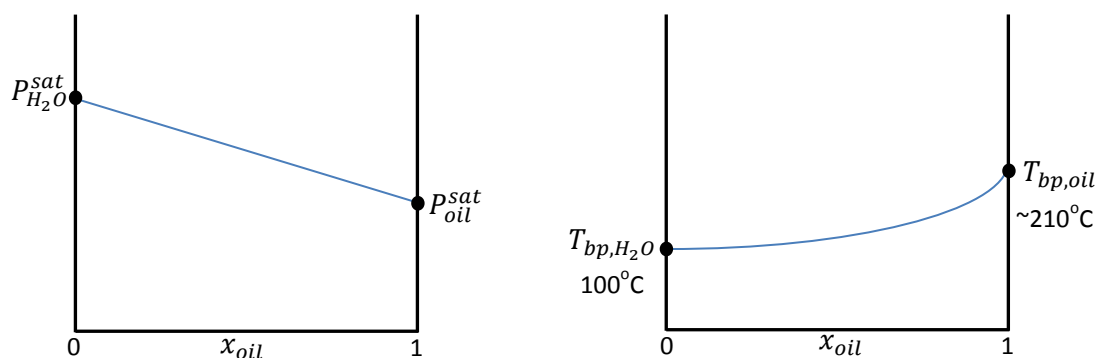


Figure 2.41 & 2.42- Raoult's law for a mixture of water and peppermint oil. (left) The vapor pressure of the mixture based on mole fraction of peppermint oil. (right) The boiling temperature of the mixture based on mole fraction of peppermint oil.

Raoult's law is only considered valid when the system is ideal and all intermolecular forces are considered the same (Koretsky 2004). This case can be considered ideal because it is treated as a dilute system; the amount of mint oil in the mixture is considered to be approximately 1% mole fraction. At 1% we can assume the vapor pressure and boiling temperature will be very close to that of water.

A diagram of the steam distillation process from the 1950s can be found in Figure 2.43 as reported by an Oregon State Field Distillation Survey (Hughes 1952).

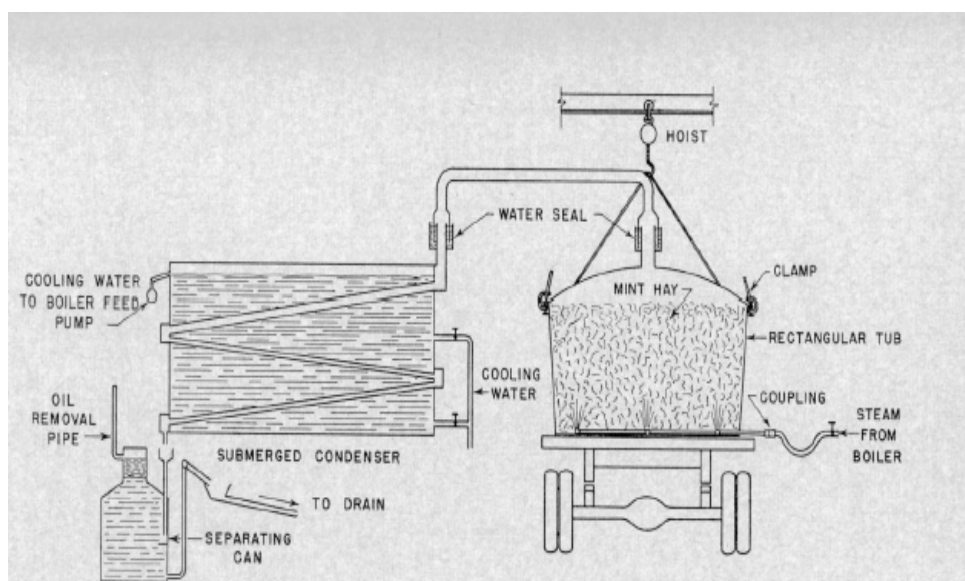


Figure 2.43- Distillation unit with a portable tub (Hughes 1952).

Since his report was published minor changes have been implemented to the process. One of these changes is the design of the condenser; a vertical tube and shell condenser has been designed with more tubes for improved efficiency.

The mint is dried, chopped, and collected in the back of a tub it is then taken for processing. A steam manifold is built into the bottom of the tub and the mint acts as a packed bed reactor. As the steam passes through the mint it breaks apart the remaining undamaged glandules and transports the mint oil out through the top. A tub will fit into a single processing bay; most farms will have 6-8 bays available. A boiler is used to produce the steam for the extraction process. Diesel and natural gas are the most commonly used fuels for the steam boilers. The steam is fed into the packed bed of mint through the manifold in the bottom of the tub. With pressure as the driving force it is driven through a tube and shell condenser. The condensate then flows into a continuous separator operating at a temperature around 115°F.

This temperature is used because it yields the highest difference in specific gravity while avoiding thermal degradation to the oil. The separators are also designed with a conical top; this is so surface tension will also play a role in the separation of the oil from water. Each tub will require about 100 boiler horsepower to produce the steam. Usually more than one tub will be run at a time; for this reason it is common to find a systems that use a 100 hp and 500 hp boiler (or two other size boilers) together. It is important to note that one mechanical horsepower refers to 745W while one boiler horsepower refers to 9810W; the amount of energy to evaporate 15.6 kg of water to saturated steam (Dictionary 2012).

A study presented by the Executive director of the MIRC, Rocky Lundy, breaks down the carbon emissions for each part of the farming and distilling process. The study includes 17 farms information from the Northwest region. Using the average carbon emissions from the 17 farms it is estimated 25.07 kg CO₂ are released for each kg of mint oil produced (Gregory 2012). Figure 2.44 shows the general sources of carbon emissions and their proportionate contributions.

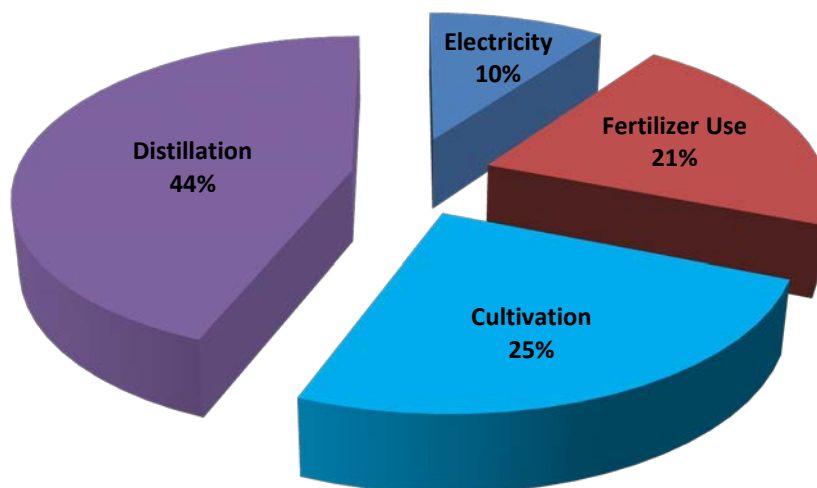


Figure 2.44- Farm activities relative contributions to total CO₂ emissions of 17 Northwest area farms (Gregory 2012).

The figure shows that almost half of the total carbon emissions come from the distillation process. Since it is estimated that steam distillation is only able to extract about 20% of the mint oil available from the peppermint leaves and extraction times take anywhere from 1.5-4.5 hours (Lucchesi 2004), an opportunistic area to focus process improvements is toward increasing efficiency and sustainability of the distillation process.

2.5 Solvent Free Microwave Extraction

Solvent free microwave extraction has been shown to be able to remove up to 65% of available oils and take anywhere from 1.5-45 minutes. SFME in comparison to steam distillation can yield up to three times the amount of oil and due to shorter processing times reduce the cost of energy (Velasco 2007, Lucchesi 2004).

In SFME mint is exposed to microwave radiation via a microwave applicator. The microwaves increase the vibrational energy in the water molecules, this continued increase in energy causes the water to boil and change phase. One main difference

between SFME and steam distillation is the source of the steam for the extraction. In SFME the steam is generated from water remaining in the leaves of the plants. This causes greater disruption of the surface of the leaves (in particular the disruption of the elevated cuticle of Figure 2.31) and is hypothesized to be one of the reasons more oil is extracted.

Scanning electron microscopy (SEM) pictures were taken before and after mint leaves were processed by the solvent free microwave method. The before and after SEM images are shown in Figures 2.51 and 2.52 respectively (Velasco 2007). The images show the peltate glandules have broken apart after the microwave process has occurred. Similar SEM images have been reported for essential oil extraction of cardamom seed. Researchers observed differences in solvent free microwave extraction from hydro-distillation, showing that cells are broken and damaged much more noticeably during SFME (Lucchesi 2007).

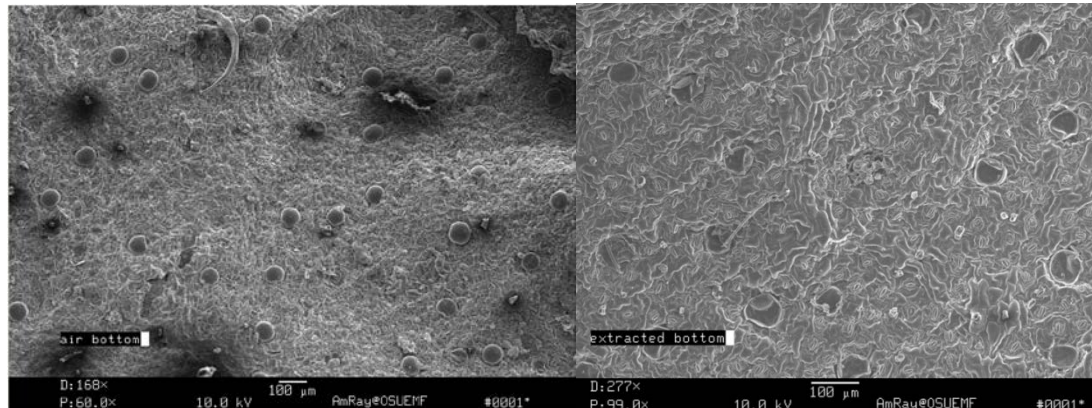


Figure 2.51 & 2.52- (left) SEM Peppermint leaf prior to microwave extraction. (right) SEM Peppermint leaf post microwave extraction (Velasco 2007).

Before this research began a field test was conducted on a pilot scale continuous microwave applicator system. Figure 2.53 shows the flow diagram for the microwave pilot plant used for the field test.

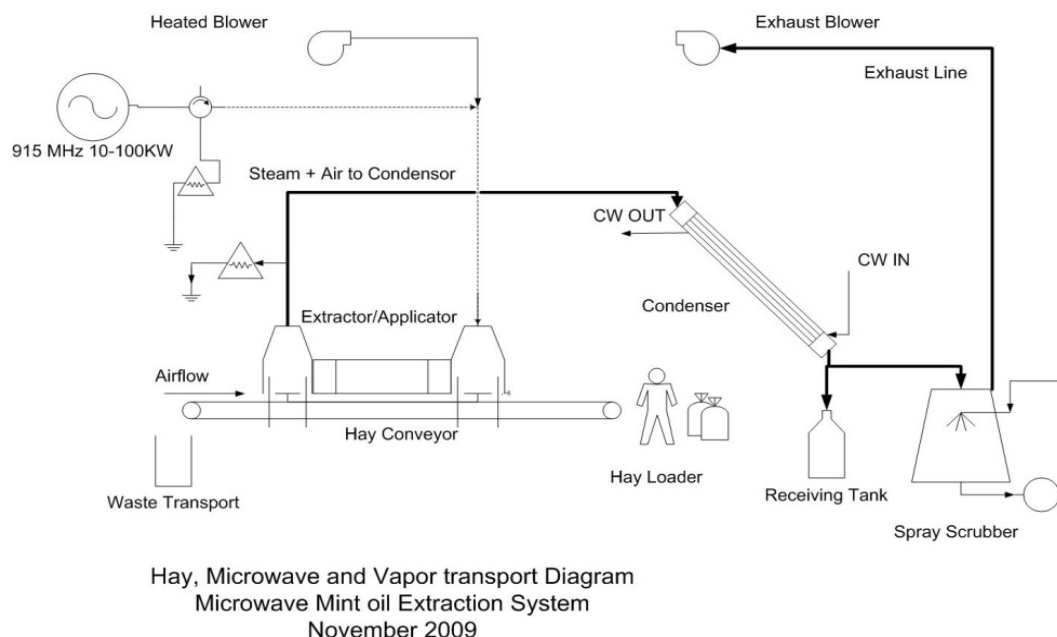
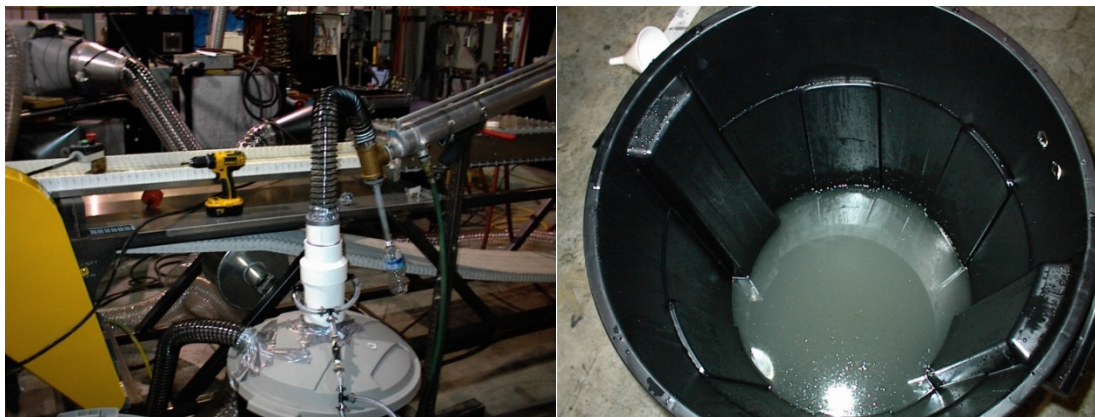


Figure 2.53- Flow sheet diagram from the North Carolina trials during November of 2009 (Hackleman 2009).

Mint hay was fed into the microwave in a four inch deep bed on a conveyor belt. A blower at the end of the process created the pressure drop that pulled extract mixture through the condenser then through the spray scrubber. A tube and shell heat exchanger was used to condense the steam and oil stream. However, the tube and shell was unable to successfully condense much of the mixture. It was determined that air was getting drawn into the stream with the steam and mint oil through the open ends of the microwave (note “airflow” on Figure 2.53). It is known that in the presence of a noncondensable vapor, tube and shell condenser performance will be greatly reduced (Collier 1981). This is due to a gas boundary layer developing as condensation is formed along the condenser tube and it is this boundary layer which resists the steam from condensing (Seunguim 2006). It is more difficult to condense because the air acts as an insulator against heat transfer. After inspecting the system the research team found the recycled flow spray scrubber had captured a significant amount of oil that had escaped the tube and shell condenser. Figures 2.54 and 2.55 show the spray scrubber and the oil captured inside.



Figures 2.54 & 2.55- (left) The design of the spray scrubber with recycle water stream. (right) The oil captured in water at the bottom of the spray scrubber (Hackleman 2009).

Microwave extraction could also change the way that farmers harvest their crop. Currently after being cut the plants must sit in the field to dry for several days to enable a chopping process to take place on the plant material. Research suggests that during this waiting time period no significant mass of oil is lost (Gershenzon 2000). However there is a significant risk of weather conditions affecting the oil in the plants. In addition, the composition of the oil is changed during this drying period. After drying the hay is then chopped and placed into large mobile trailers called mint tubs for processing. The microwave system requires a higher moisture content in the mint hay than steam distillation during processing or ignition and combustion can take place. Table 2.51 shows some of the power ratings and belt speeds used for the microwave experiments in North Carolina.

Table 2.51- Data for experimental conditions on 11/16/09 follows (Hackleman 2009).

<u>Run</u>	<u>Belt Speed</u> FPM	<u>Power</u> KW	<u>Duration</u> Min	<u>Outgoing</u> °C	<u>Comments</u>
1	10	20	1	40	Pre-heat air
2	10	35	2	60	1/2 Pre-heat air
3	6	35	2	50	No pre-heat
4	5	35	2	58	No pre-heat
5	3	35	6	Fire	Ignition at 30s
6	3	25	6	58	Cleaned condenser prior
7	2.5	25	10	72	Operated well
8	2.3	25	8	Fire	smoke at 4 min

Slow belt speeds and higher power rating resulted in higher outgoing temperatures and in some cases combustion. Note the outgoing temperature shown in Table 2.51 is measured beyond the end of the microwave applicator due to the design of the system. The mint hay and vapors leaving the system are actually above 100°C. The mint collected for these experiments was taken from a farm after it had been chopped and dried for steam distillation. To avoid combustion, additional water had to be sprayed onto the mint before passing it through the microwave. More testing is needed however this implies that mint may be able to cut and immediately processed via SFME.

3. Materials

3.1 Steam Generation Hood

A steel hood was used to generate the steam air mixture at different ratios. The hood was fitted with a single speed blower to draw the mixture into the condenser. Small holes were drilled into galvanized steel pipes to deliver steam into the hood and act as a manifold for even distribution. The steam was plumbed into the system from the University's heating pipeline which delivers saturated steam at roughly 60 PSI. By adjusting a room ambient air gap between the manifold and the hood, it was possible to enable emulation of the stream conditions delivered from the microwave pilot plant. The noncondensable air stream entered the system through this gap. The steam to air ratio could be altered by either changing the flow rate of steam via steam pressure at the inlet or by increasing the area open to the atmosphere. The dimensions of the steam hood were 27.5" x 42" and are illustrated in Figure 3.11. A flexible rigid aluminum heating duct was used to connect the hood to the rest of the condenser.

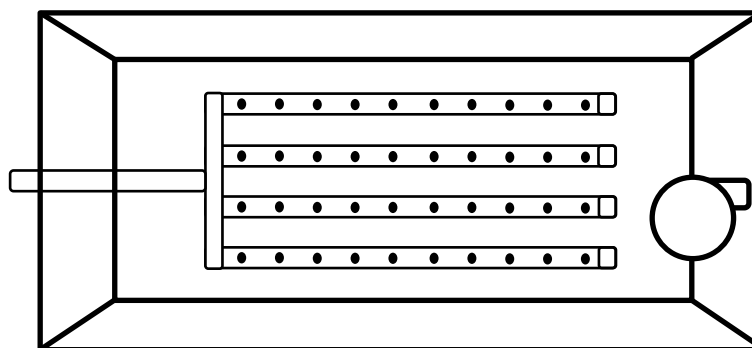


Figure 3.11- The steam hood with steam manifold inside. Note: steam manifold is not to the exact scale as the hood.

3.2 Direct Contact Condenser

Aluminum and stainless steel 316 were selected as the most suitable materials due to their anti-corrosive nature to high temperature steam and peppermint oil (De Renzo 1985). Aluminum heating ducts were assembled to act as the center column of the condenser. The center column consisted of three parts; a 4" duct connected to a 6"

duct via a 4"-6" reducer. Holes were drilled into each section of the center column to fit the spray nozzles. Eight nozzles were fitted into the 4" section, four nozzles were fit into the reducer, and four nozzles were fit into the 6" section. The aluminum shell was manufactured from design drawings created by this author by RJH Enterprises. The shell was designed to hold an additional eight nozzles and support the center column. A schematic of the condenser can be seen in Figure 3.21. The full specifications for the shell are in Appendix A.

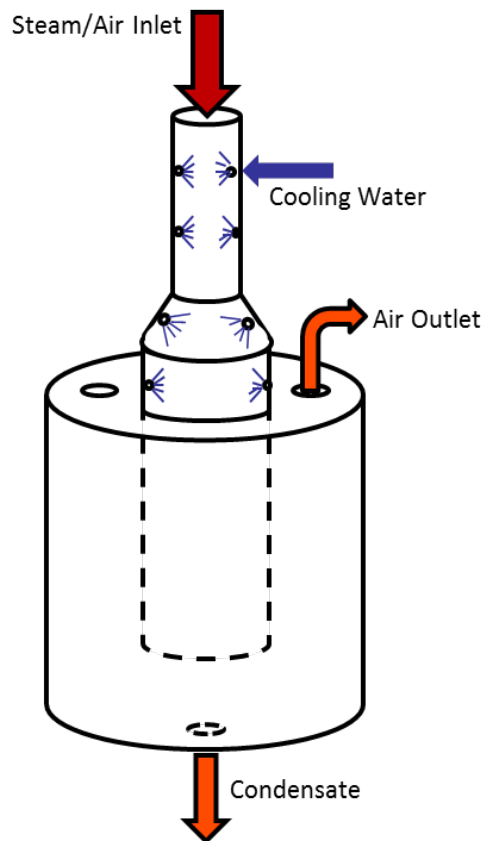


Figure 3.21- The design of the direct contact condenser used in this experiment. Note that the figure does not show the correct number of nozzles, the shell nozzles, or the mounted ring. See appendix A for full shell specifications.

The center column fits into the shell and is resting on a ring mounted in the bottom of the condenser. This allows for added stability and reproducible experiments because it fixes the dimensions of the spray column. It also allows for water to reside in the bottom of the vessel without blocking the air flow out of the center column. Figure 3.22 is an image of the condenser connected to the hood in the configuration used for testing.



Figure 3.22- The aluminum condenser attached to the steam generation hood.

3.3 Nozzles

Stainless steel nozzles were selected based on their flow rate and spray angle. A 120° fan spray was chosen because it would spread out the coolant to cover the largest area. The number of nozzles and spray flow rate was determined based on an energy balance assuming a 100kW microwave applicator would be running at power levels of 25-65kW. This was chosen because data taken from the pilot plant experiments indicated this was the working range of the system.

The volume of liquid necessary to cool the system is calculated by the amount of energy that is transferred to the coolant water. Equation 3.31 was used in this calculation. The kW represents the power output of the microwave unit to be simulated. One can assume that the energy needed to be removed from the system will be no more than the amount of energy entering via microwave radiation. In this case we assume that the steam/air stream and the coolant water will reach an equilibrium temperature in the condenser.

$$kW = n_{nozzles} m_{coolant} C_{p_{water}} (T_{exhaust} - T_{mix}) \quad (3.3.1)$$

Rearranging and selecting the desired amount of energy to remove in kW we can solve for the number of nozzles needed. Equation 3.32 shows how the number of nozzles was estimated where $m_{coolant}$ is the flow rate of each nozzle. Appendix C has the performance of Lechler® nozzles similar to the nozzle type chosen for this experiment.

$$n_{nozzles} = \frac{kW}{m_{coolant} C_{p_{water}} (T_{mix} - T_{coolant})} \quad (3.3.2)$$

Figure 3.31 shows the number of nozzles needed assuming a water pressure of 40 PSI to attain a 0.6 GPM flow rate over various cooling water temperatures. The spray flow rates of the nozzles used in this calculation are highlighted in Appendix C; these are the same nozzles used in this research. The plot uses Equation 3.31 and assumes a maximum of 65kW will need to be removed from the system to cool the mixture.

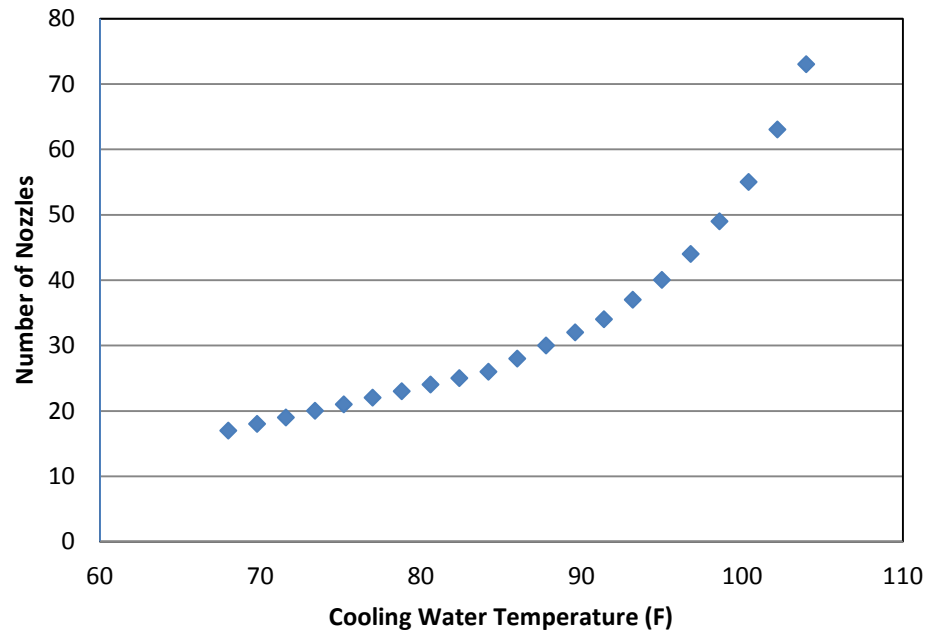


Figure 3.31- Number of nozzles needed assuming 65kW max removal and 0.6 GPM Lechler® nozzles at 40 PSI.

4. Methods

4.1 Experimental Design

The experiments were designed to determine the efficiency of the condenser based on its ability to capture the incoming steam in the steam-air mixture. The temperatures of the incoming and exiting steam/air stream were measured to determine the mass ratios of both streams. An anemometer was used intermittently on the exit stream to determine the velocity of the stream leaving the mixture. The anemometer was not designed to be attached to the condenser but the velocity can be interpolated between measurements. Aspen HYSYS was used to model the mixing of 100°C steam and 20°C ambient air and was recorded over a range of changing mass ratios using the Peng-Robinson correlation (Koretsky 2004). It is important to note that Equation 4.1.1 only accounts for one component while Aspen HYSYS accounts for multiple.

$$P = \frac{RT}{v - b} - \frac{a\alpha(T)}{v(v + b) + b(v - b)} \quad (4.1.1)$$

Figure 4.11 shows the Aspen HYSYS results for this mixing temperature based on % steam by mass in the generation hood.

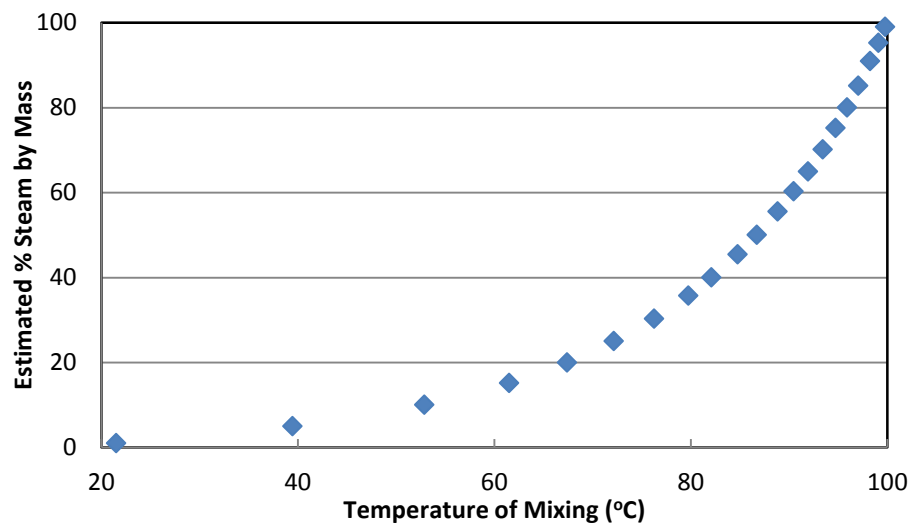


Figure 4.11- Aspen HYSYS results for mixing temperature based on % steam by mass.

The condenser was placed inside a chemical spill containment vessel to act as a reservoir. The reservoir with condenser where then placed on top of an industrial barrel scale to measure the mass of water condensed. At the beginning of each experiment the reservoir was filled with fresh coolant water at approximately 20°C. Once the system was prepped by connecting all of the instrumentation the steam was turned on. The steam was run through the generation hood and condenser until it reached the desired steady state temperature. At this point the pump was turned on and the computer measurements of the system were taken. The computer logged the inlet, reservoir, and outlet temperatures as well as the velocity exiting the condenser; however this was not fully automatic since the anemometer had to be placed over the exit for each measurement. Mass measurements were recorded manually by reading the scale every minute. The full flow diagram for the process with instrumentation can be seen in Figure 4.12.

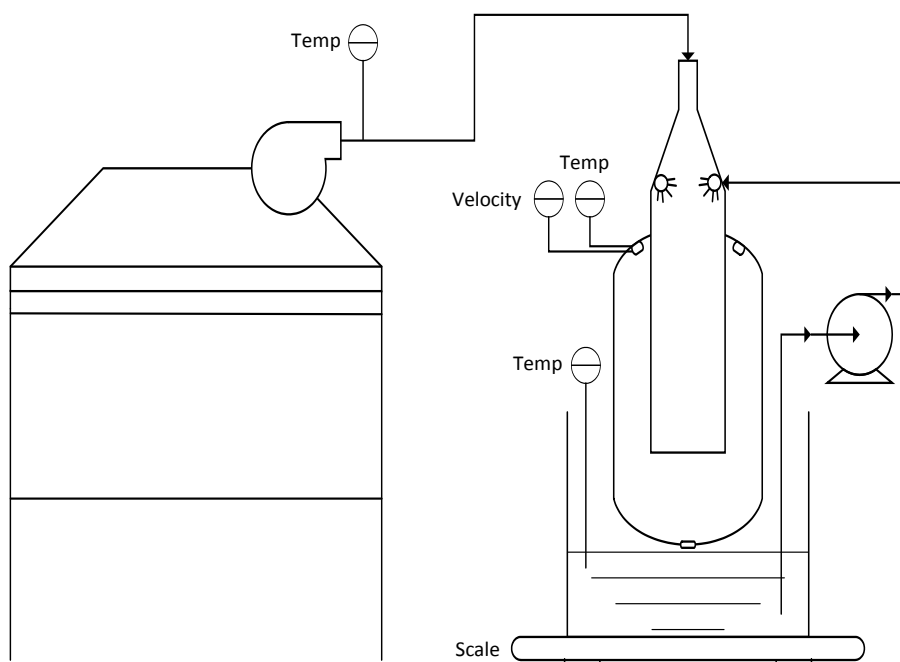


Figure 4.12- The flow diagram for the experimental set-up to test the condensers efficiency.

4.2 Material Balance

A material balance was needed to determine the incoming flow rate of steam into the system. The velocity of the stream leaving the condenser was measured to determine the mass flow out of the system. Using this velocity a volumetric flow rate can be calculated. Equation 4.2.1 accounts for two exhaust ports exiting the condenser and is measured in m^3/s .

$$V_{out} = v_{out}2\pi R^2 \quad (4.2.1)$$

However this mass flow is a mixture of air and noncondensed water vapor. The exiting temperature can be used to determine the saturation vapor density of the mixture. In this case it is safe to assume that the exiting stream will be at 100% RH because the air entering the condenser was saturated or super-saturated at a higher temperature. Relative humidity data was used to construct a saturation vapor density plot. Two empirical formulas were best fit to the data; one from 0°C to 50°C and the other from 50°C to 100°C . Two 3rd order polynomials were created to maximize fit while minimizing the degree of polynomial needed over the desired temperature range. Figure 4.21 shows saturation vapor density of water in air.

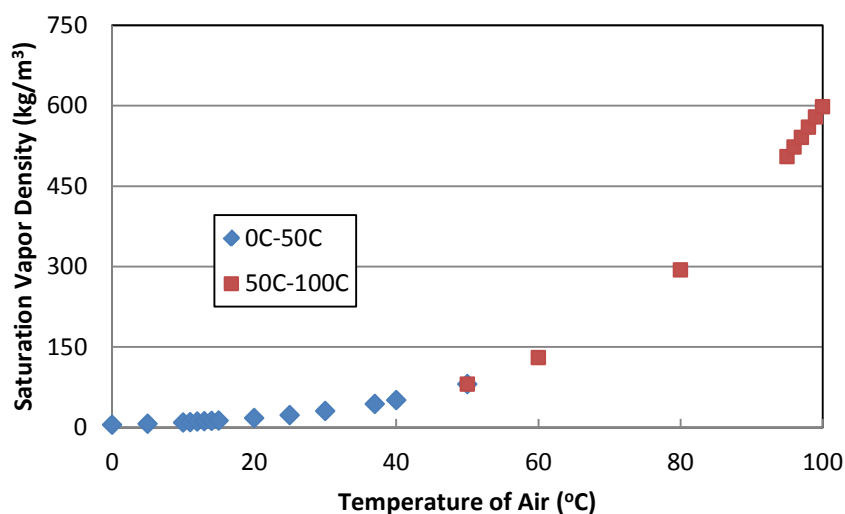


Figure 4.21- Saturation Vapor Density of water in air from 0°C to 100°C .

Equations 4.22 and 4.23 represent the saturation vapor density of air for 0°C to 50°C and 50°C to 100°C respectively.

$$\begin{aligned}
 &\text{Saturation Vapor Density (kg m}^{-3}\text{)} \\
 &= 3.124 * 10^{-7}(T(K) - 273)^3 + 8.180 * 10^{-6}(T(K) - 273)^2 \\
 &+ 3.232 * 10^{-4}(T(K) - 273) + 5.018 * 10^{-3}
 \end{aligned}
 \tag{4.2.2}$$

$$\begin{aligned}
 &\text{Saturation Vapor Density (kg m}^{-3}\text{)} \\
 &= 1.399 * 10^{-6}(T(K) - 273)^3 - 1.592 * 10^{-4}(T(K) - 273)^2 \\
 &+ 9.742 * 10^{-3}(T(K) - 273) - 1.831 * 10^{-1}
 \end{aligned}
 \tag{4.2.3}$$

Multiplying the volumetric flow by the saturation vapor density of the exhaust stream will yield the vapor exiting the system in kg/s.

$$\dot{m}_{\text{vapor-out}} = \dot{V}_{\text{out}} \rho_{\text{sat}}(T_{\text{out}})
 \tag{4.2.4}$$

The conservation of mass allows us to write the Equation 4.2.5. This states that water only exits the system as water vapor trapped in air and condensate.

$$M_{\text{steam-in}} = M_{\text{vapor-out}} + M_{\text{water-condensed}}
 \tag{4.2.5}$$

Again Aspen HYSYS was used to determine the density of the mixture as a function of its mixing temperature. We assumed a mixture of 20°C air and 100°C steam for this computation.

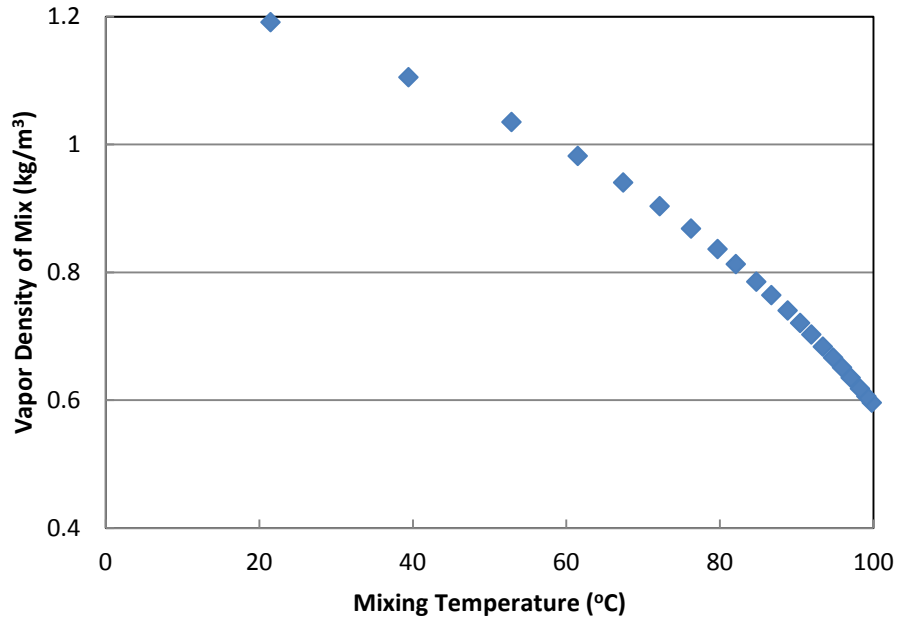


Figure 4.22- Aspen HYSYS results for density of inlet mixture based on 100°C and 20°C air.

The amount of water condensed from the steam is measured using the industrial barrel scale underneath the reservoir. The change in the reservoir is calculated by Equation 4.2.6 and measured in kg/s.

$$\dot{m}_{condensed} = \frac{dMass}{dt} \quad (4.2.6)$$

Equations 4.2.7 and 4.2.8 were solved to determine the efficiency by using the mass conservation equation to determine the amount of steam into the system.

$$\frac{\dot{m}_{H_2O-in} - \dot{m}_{H_2O-out}}{\dot{m}_{H_2O-in}} \cdot 100\% = \% Efficiency \quad (4.2.7)$$

$$\frac{\dot{m}_{H_2O-capt}}{\dot{m}_{H_2O-in}} \cdot 100\% = \% Efficiency \quad (4.2.8)$$

Using the mass of steam entering the system the velocity entering the condenser was solved. The velocity of the mixture into the system is determined by the single speed fan and the condensation of vapor in the condenser. It is not something that we are able to set, however we are interested in knowing the velocity to help characterize the system. Equations 4.2.9 and 4.2.10 show how the velocity can be determined from the mass of steam into the system.

$$\dot{m}_{total-in} = \left(\frac{100}{\%_{steam-in}} \right) \dot{m}_{steam-in} \quad (4.2.9)$$

$$v_{in} = \frac{\dot{m}_{total-in}}{\rho(T_{mix})} \frac{1}{\pi R^2} \quad (4.2.10)$$

Figure 4.23 shows the block flow diagram used in this material balance. The liquid phase leaving the system was assumed to have condensed after mixing and never entered the system.

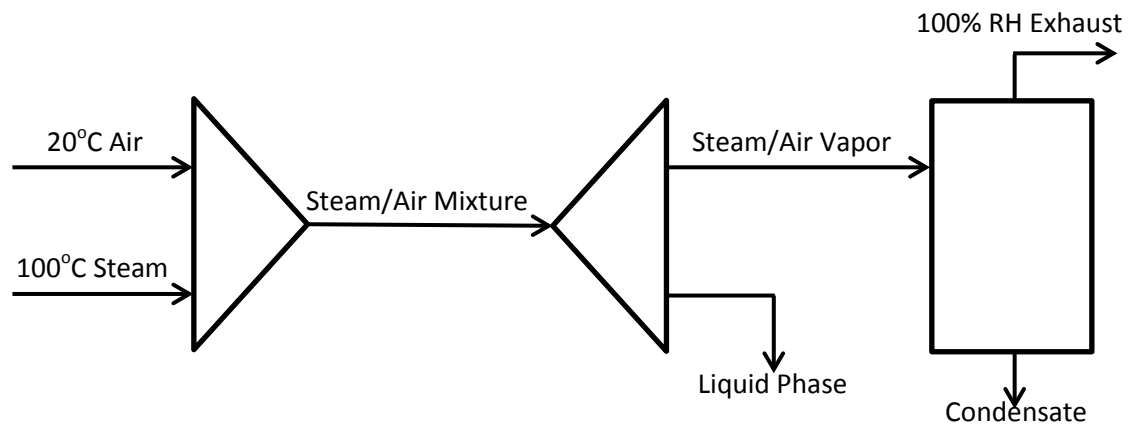


Figure 4.23- Flow block diagram for material balance of direct contact condenser

4.3 Maximum Efficiency

The maximum theoretical efficiency was determined assuming that no air gets condensed in the system and all air leaves at 100% humidity. The saturation vapor density equations were used to determine the amount of steam left in the air. For this experiment 115°F (46°C) was chosen for the exiting temperature of the condenser because farmers use this as the separation temperature of their condensers. Figure 4.31 plots the maximum theoretical efficiency for several exit temperatures.

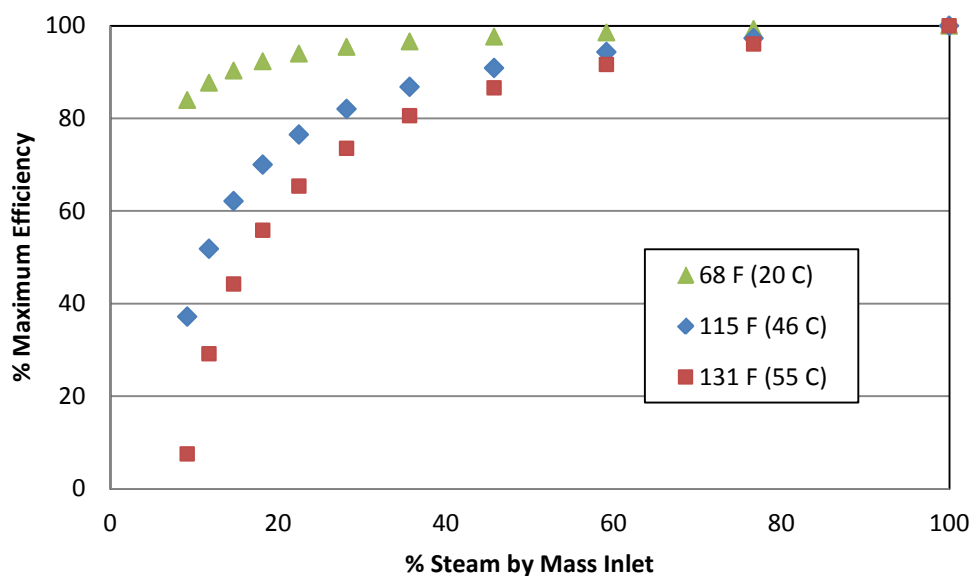


Figure 4.31- Theoretical maximum efficiency of any condenser for three different exhaust temperatures at 1 atm.

At 115°F peppermint oil and water have the largest difference in specific gravity without compromising the composition of the oil. It is possible to achieve an overall higher recovery by lowering the exiting stream temperature of the condenser.

However, additional energy would need to be removed and then added to the system to return the mixture to its optimum separation temperature. An economical analysis would need to be completed to determine if the additional mint oil saved is worth the extra cost of energy.

5. Results

5.1 Temperature Profiles

Initially it was desired to test out the condenser under a full load of 24 nozzles.

Unfortunately, the locations of some of the nozzles caused the air stream to blow out a significant amount of non-vaporized water. It was then decided that the first sets of experiments would use only the 16 nozzles in the center column. All of the experiments were run for up to 22 minutes, then the data was evaluated only over a range where the temperature of the exiting stream was at or below 115°F (46°C). An example of the exhaust and coolant temperature for a 16 nozzle test can be found in Figure 5.11. A rapid increase in coolant temperature can be noticed at the very beginning of the run; this can be attributed to warm coolant water from previous runs still in the pump.

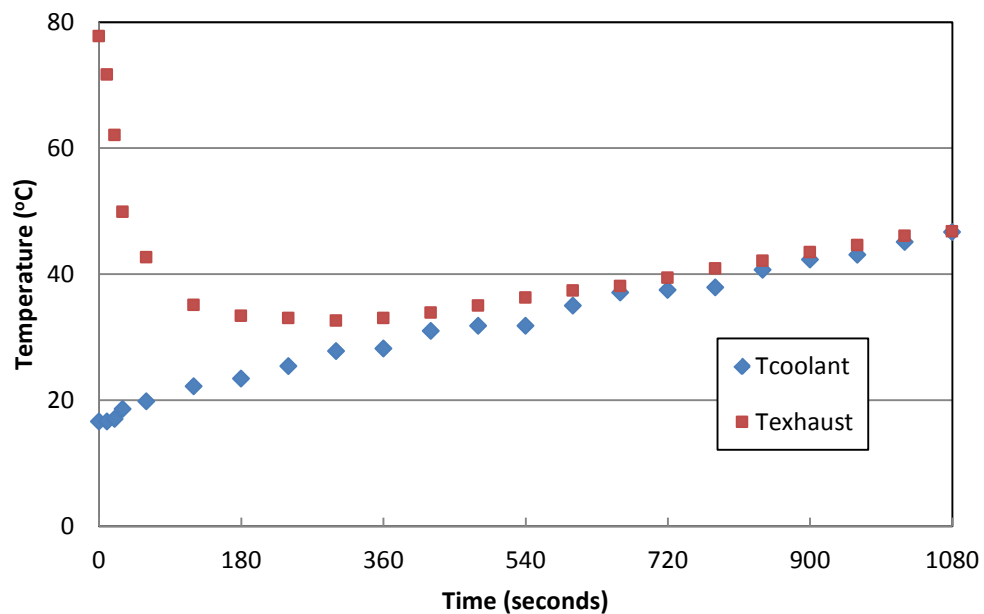


Figure 5.11- The coolant and exhaust temperatures for a 16 nozzle direct contact condenser efficiency test. The average incoming temperature for this test was 85°C.

Figure 5.12 shows the temperature profiles for the exhaust and coolant for an eight nozzle test.

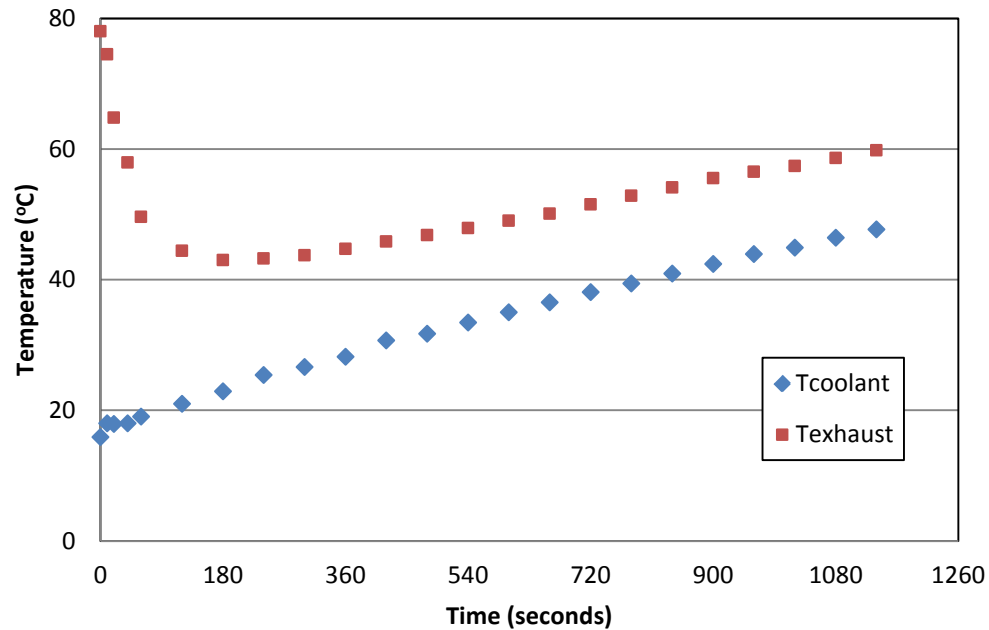


Figure 5.12- The coolant and exhaust temperatures for an 8 nozzle direct contact condenser efficiency test. The average incoming temperature for this test was 82°C.

In comparison to Figure 5.11 we can see that the eight nozzles cool the inlet less thus there is a larger difference between the two streams. The coolant water reaches the same temperature over the same amount of time (46°C over 1080s) but doesn't cool the exiting stream as efficiently. To test eight nozzles a pressure bypass valve was implemented to enable the pump to operate above its minimum stable flow regime, thereby also stabilizing the applied pressure to the nozzle set.

5.2 Efficiency Results

Equations 4.2.10 and 4.2.11 were used to determine two efficiencies which were then averaged for each data point. Figure 5.11 shows the results of the direct contact condenser plotted against the maximum theoretical efficiency at a 115°F stable operation temperature.

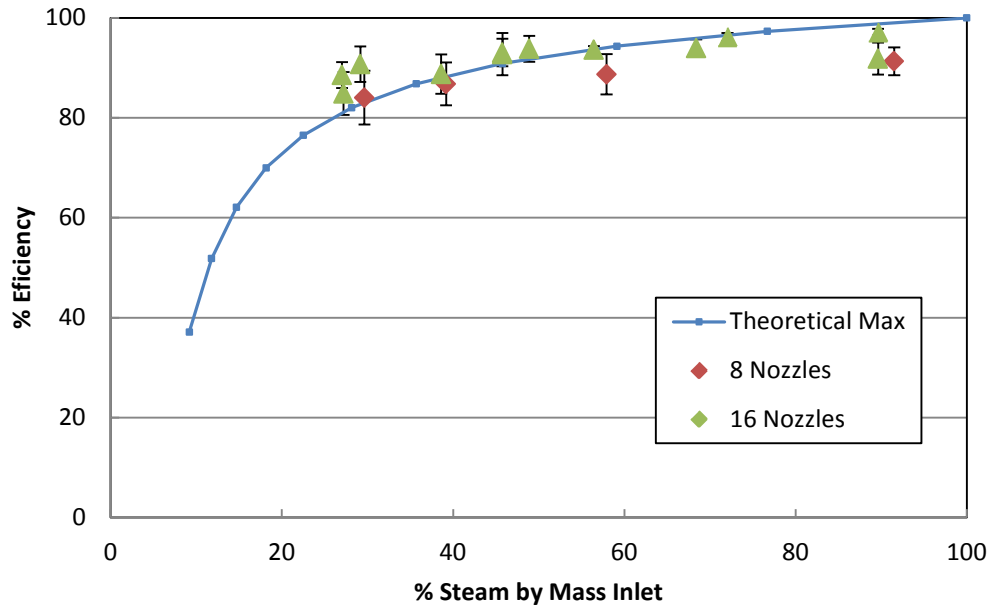


Figure 5.21- The measured efficiencies plotted against the theoretical maximum for 8 and 16 nozzles.

The 16 nozzles follow the theoretical efficiency but appear to fall slightly below the maximum at the highest steam ratios. This is because at the highest steam ratios there will be more energy to remove than the maximum capacity of the condenser can handle. The 8 nozzles trend the same way but as one would expect with using less coolant you would be able to condense less steam.

5.3 Condenser Capacity

We are also interested in determining the amount of energy removed by the coolant water; this is known as the condenser's capacity. Equation 5.3.1 was used to determine the condenser's capacity to remove energy from the system for each 16 nozzle test.

$$kW = m_{steam}\Delta H_{vap} + m_{H_2O}Cp_{H_2O}(T_{mix} - T_{out}) + m_{air}Cp_{air}(T_{mix} - T_{out}) \quad (5.3.1)$$

The first term of the equation is for the energy to condense the steam from a vapor to a liquid. The second term is for the cooling of water from its boiling temperature to its exit temperature, and the third term is for the energy removed from air to cool it from

the mixing temperature entering the system to its exit temperature. Figure 5.31 shows the results of condenser capacity.

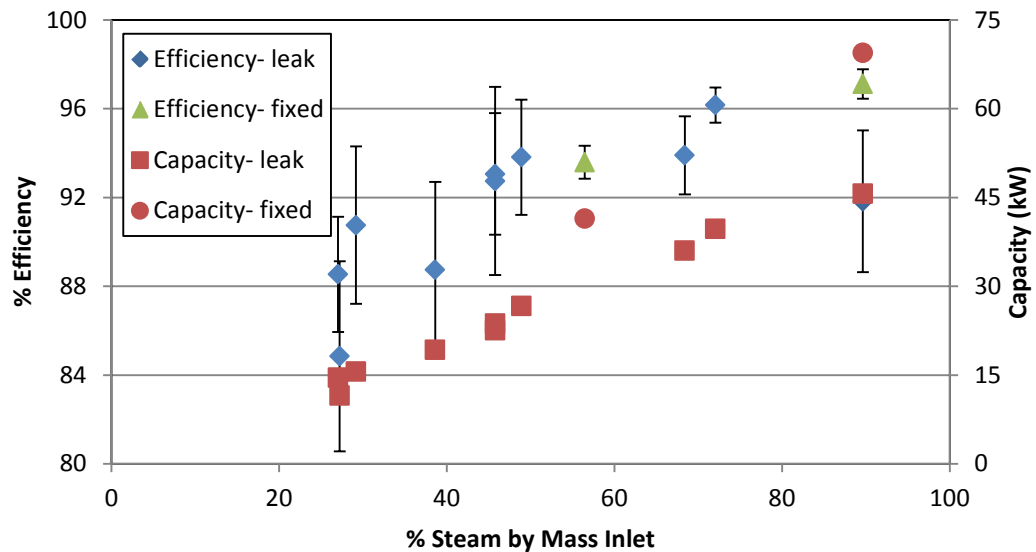


Figure 5.31- The average efficiency for 16 nozzles taken from Figure 5.21 shown with the calculate condenser capacity (energy removed). Note the efficiency axis ranges from 80-100%.

5.4 Scale Up

It is possible to scale up the condenser by increasing the flow rate of coolant spray. Two ways to increase the flow rate of spray coolant are to increase the number of nozzles or to increase the pressure of the coolant stream. Figure 5.31 shows the different number of nozzles required depending on the temperature of the coolant water assuming 40 PSI. Figure 5.41 assumes that we are using the Lechler® nozzles found in Appendix C. The plot assumes removal of 65kW energy from the steam/air stream. We would also want to have the same velocity or residence time of steam/air mixture in the condenser. We can accomplish this by increasing the diameter of the center column of the condenser.

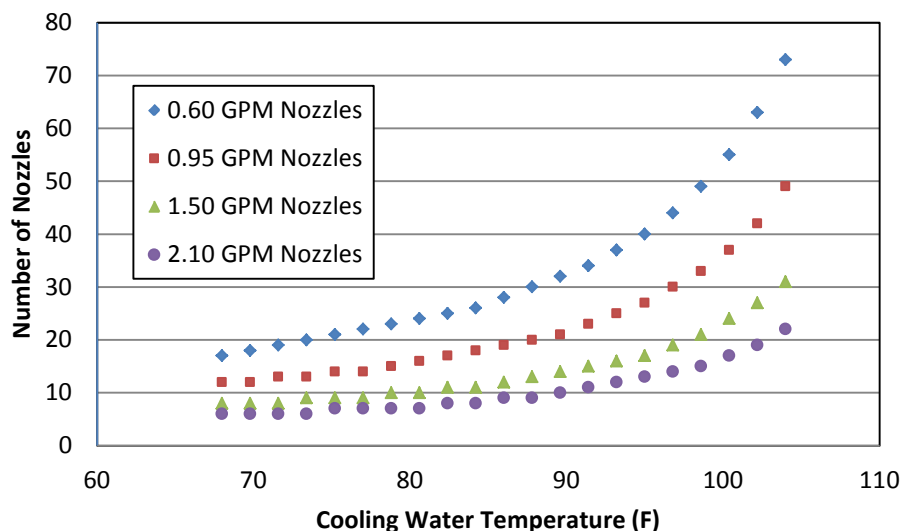


Figure 5.41- The number of nozzles required according to equation 3.3.2 for different coolant water temperatures and nozzle flow rates.

When scaling up it is important to note that there will be a greater mass of steam/air entering the system. This will also cause an increase in velocity and require a larger inlet to the condenser. Steam traveling too fast will not have adequate time to be cooled and condensed in the system and be lost. The diameter of the inlet to the condenser needs to be increased to enable the appropriate residence time range to be retained.

5.5 Velocity of gas

More testing is required to determine the effects of the inlet stream velocity. Because the blower runs at a single speed it's impossible to change the velocity for different temperatures. Instead the velocity is partially a result due to the pressure drop from the condensing steam in the mixture. At higher steam ratios and efficiencies there is a greater drop in pressure and a larger flow rate. The velocity of the inlet steam/air stream was calculated using the air flow rate out of the system and the percent steam by mass entering. At one point during the experiment a new outlet fitting was attached to the steam hood to fix a leak. This fix resulted in higher velocities and

mass flow rates into the condenser. Figure 5.51 shows the gas inlet velocities for 8 and 16 nozzles.

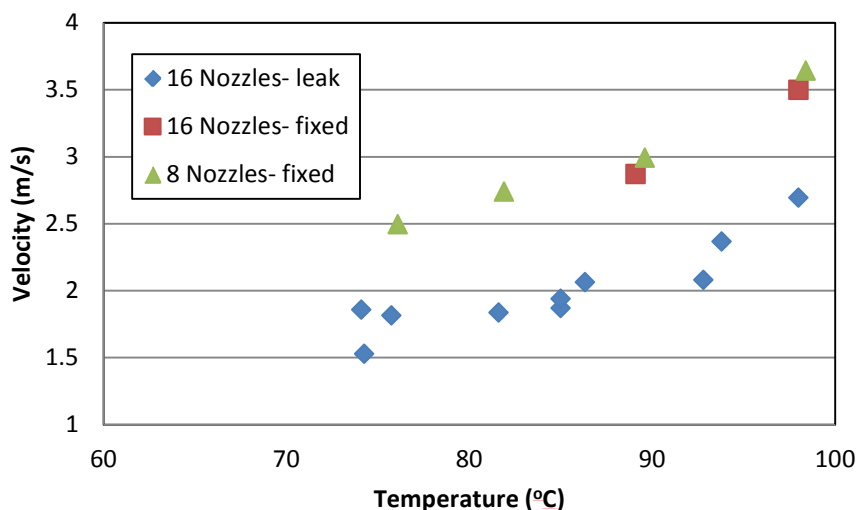


Figure 5.51- Average velocity of steam/air mixture into the condenser. (Each experimental point is derived from the average of roughly 20 separate measurements. Overall precision and accuracy of measurements is reflected in the variation seen in this figure.)

5.6 Separation

There can be an issue with losing more of the product in the coolant. With the added volume of coolant to the mint oil and water condensate there will be a greater loss of oil due to solubility. If a coolant water recycle was implemented farmers would lose approximately the same amount of oil as in the current steam distillation process. This would be due to loss of oil in the purge stream. Once the water reached its maximum oil solubility there would be a steady state oil flow out of the system. The initial oil lost into the coolant's volume could remain in the system to avoid a large loss every year or day. Section 7.3 outlines two separate approaches to coolant water recycle that will solve this issue of oil loss. A literature search was conducted to find the solubility of peppermint oil in water (Storer 1864). The only information yielded by a literature search was that it is "sparingly soluble" in water.

6. Conclusions

Steam distillation is the traditional method used for the extraction of peppermint oil. This process is able to remove approximately 20% of the oils from the leaves of the plant. It is a very costly and un-sustainable process due to the release of carbon emissions. Solvent free microwave extraction promises yields of up to 65% of the available oils from the peppermint at 3% less cost (Velasco 2007). It will also reduce carbon emissions because it will be using electricity as a power source instead of fossil fuels and electricity can be generated from fully sustainable, carbon emission free energy sources. In 2009 a SFME pilot plant was assembled in North Carolina to test the efficiency of the microwave process on a larger than lab scale. Results from the experiments showed that the tube and shell condenser was unable to effectively condense the mint oil. The problem was determined to be the addition of air to the mixture due to the open ends of the microwave. However it was discovered that the spray scrubber after the condenser was able to collect a visible amount of oil. This inspired the design of a direct contact condenser by Pommerenck et al. Due to the materials used in the manufacturing of this condenser, it could not be tested at the conditions found in the microwave pilot plant. The direct contact condenser they designed did show vast improvements in steam capturing efficiency when compared to a tube and shell condenser. A direct contact condenser was designed based on the design proposed by Pommerenck et al. It was constructed out of aluminum with stainless steel spray nozzles for their non-corrosive properties. Tests were conducted using 8 and 16 nozzles and tested over a range of 20-100% steam by mass. Additional tests were completed using 24 nozzles but due to the location of some of the nozzles coolant was lost as an aerosol with no way to measure how much. Figure 6.11 shows the results of the 8 and 16 nozzle tests compared to the tube and shell results as reported by Pommerenck. Error bars show the standard deviation for the average calculated efficiencies. Due to the difficulty of reproducing exact experimental conditions, efficiencies were averaged over a non-steady state period. This large fluctuation of exiting temperatures causes larger error bars on some data points.

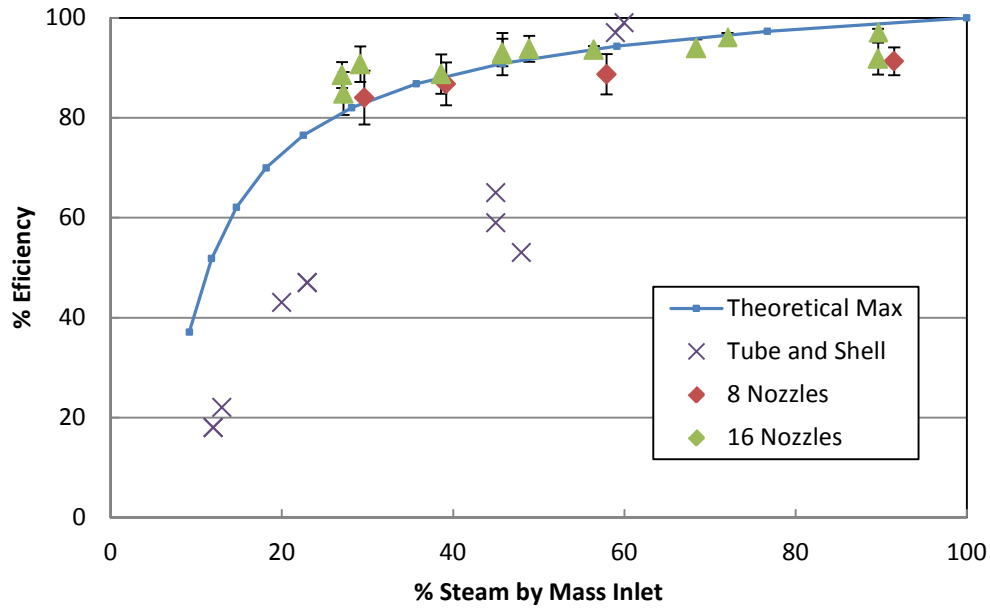


Figure 6.11- The shell and tube data points reported from Pommerenck et al. for a constant flow rate but a different type of nozzle.

As the mass of air in steam is increased a drastic decrease in the efficiency of the tube and shell condenser is seen. This is because air insulates the tube and shell condenser by forming a barrier boundary layer that resists heat transfer and condensation. The capacity of the condenser ranges from 10-50kW depending upon the amount of energy entering the system. This agrees with the amount of energy that enters the system due to the microwave. This research shows that a direct contact condenser is more efficient and can be designed and scaled up to the design specification of a larger plant.

The tube and shell data reported by Pommerenck uses a flow rate of 24 L/min of coolant water. To compare this to the data from this research we calculate the equivalent number of nozzles. Each nozzle is specified at 40 PSI to expel 0.6 GPM of water. Equation 6.1.1 is used for this calculation:

$$n_{nozzles} = 24 \frac{L}{min} \left(\frac{1}{3.79} \frac{gal}{L} \right) \frac{nozzle}{0.6 gal} \quad (6.1.1)$$

When compared to the nozzle and pump used in this experiment it represent an equivalent of 10.5 nozzles in operation. Figure 6.11 shows data for 8 nozzles which well exceeds the tube and shell condenser's performance at lower ratios of % steam by mass.

7. Future Work

7.1 Direct Contact Condenser Field Test

Due to unfortunate circumstances a field pilot plant test scheduled at the North Carolina facility were cancelled. This was because the company was being sold at the time we had planned to go test the condenser. There is still an interest in finding another place that has a microwave system where we can test the condenser. However this will most likely be the next person working on this project.

7.2 Direct Solar Generation

Additional areas were explored as means of increasing sustainability by means of reducing carbon emissions. One of these was the supplementation of the gas boilers by direct solar generation (DSG). We wanted to utilize the amount of solar irradiance that hits the Willamette Valley during the mint distillation season. Figure 7.21 shows the solar irradiance on August 1st for Junction City, Oregon.

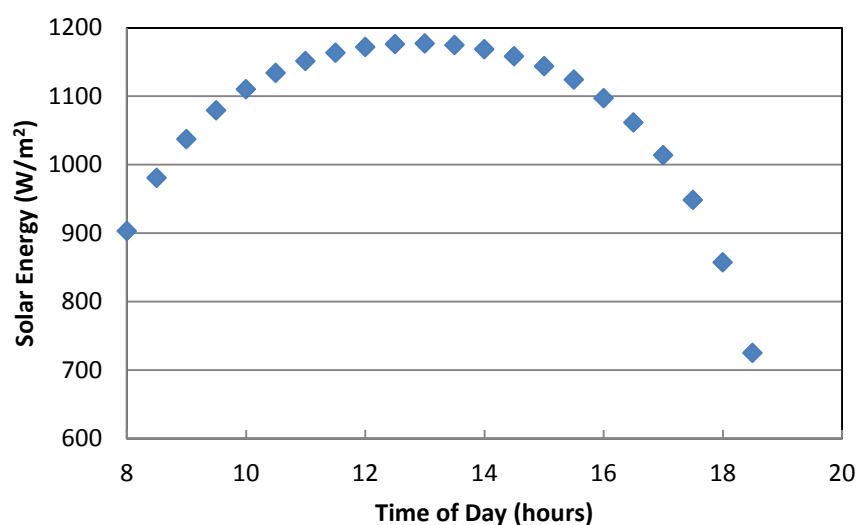


Figure 7.21-Solar irradiance over Junction City Oregon, August 1.

The mint distillation season lasts 4-6 weeks, is centered on August 1st and does not change greatly +/- 3 weeks. DSG uses concentrating mirrors to focus sunlight onto a small surface of a pipe. Inside the pipe water is heated and is turned into steam, the

steam is then forced into a generator where it produces electricity. One of the benefits of this process is the extra steam it creates during the entire year will be able to produce electricity which can be sold back to the electric company at wholesale value. The idea would be to utilize energy from 8:00 AM to 5:30 PM when the Willamette Valley is receiving at least 900 W/m^2 . The reported efficiencies for such a process are 65% solar to steam conversion and 15% solar to electric conversion (Eck 2006). Using this information it would cost \$17M to build a 5MW solar to electric DSG plant. It would require about 9 acres of space for the mirrors; the price includes both the costs of mirrors and steam to electric generators. Figure 7.22 shows the flow diagram for the proposed system.

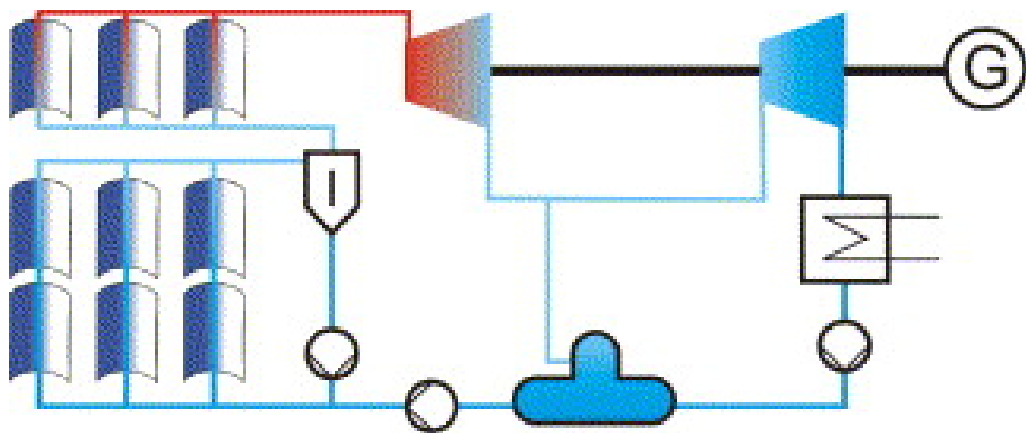


Figure 7.22- Flow diagram for the superheated direct solar steam generation process (Eck 2006).

Assuming that the process would be able to run 1900 hours a year and sell the electricity back at \$50/MWh they could generate \$500k a year through electric sales. These estimates are based on reported costs, and consequently can be subject to dramatic change. The estimation presented here does not seem economically viable without significant reduction in the capital investment. We could also propose just the mirrors to reduce fuel costs. To replace a 100 or 500 hp boiler it would require 1/3 acre and \$400k or 2 acres and \$2M, for the mirrors alone respectively. This would be able to supply just the steam needed and additional unknown capital would be required to add steam to electric generators for the rest of the year.

7.3 Coolant Water Recycle

Another area that could reduce environmental impact and increase sustainability is coolant water recycle. There are currently few clearly defined guidelines for mint farmers on disposal of the water after it has been separated from the oil. In fact many farmers in the past have just dumped the hot liquid into an open to air pond to cool. This is a very energy wasteful practice. Well and stream water expelled this way may have mint oil at its solubility limit. It is often utilized as an irrigation water source. If the water could be cooled and re-used it would allow for less of an impact on the environment, both in water use and in that low concentration of mint oil contained within. This “floral water” leaking into streams can be detrimental to fish populations if at a high temperature. Many streams in the northwest area harbor salmon and many mint farms exist in the watershed of these streams. It is against ESA regulations to affect the water temperature or composition in these areas (Jenkins 2012).

Two main ways of coolant recycle have been proposed. The first is the storage of coolant water in a large container that can sustain an entire days’ worth of coolant. At night when the ambient temperature drops, the coolant can then run through a forced convection air radiator. This process will require a larger area for the coolant to be stored but have a smaller energy cost. Figure 7.31 is the coolant flow diagram for the large storage tank.

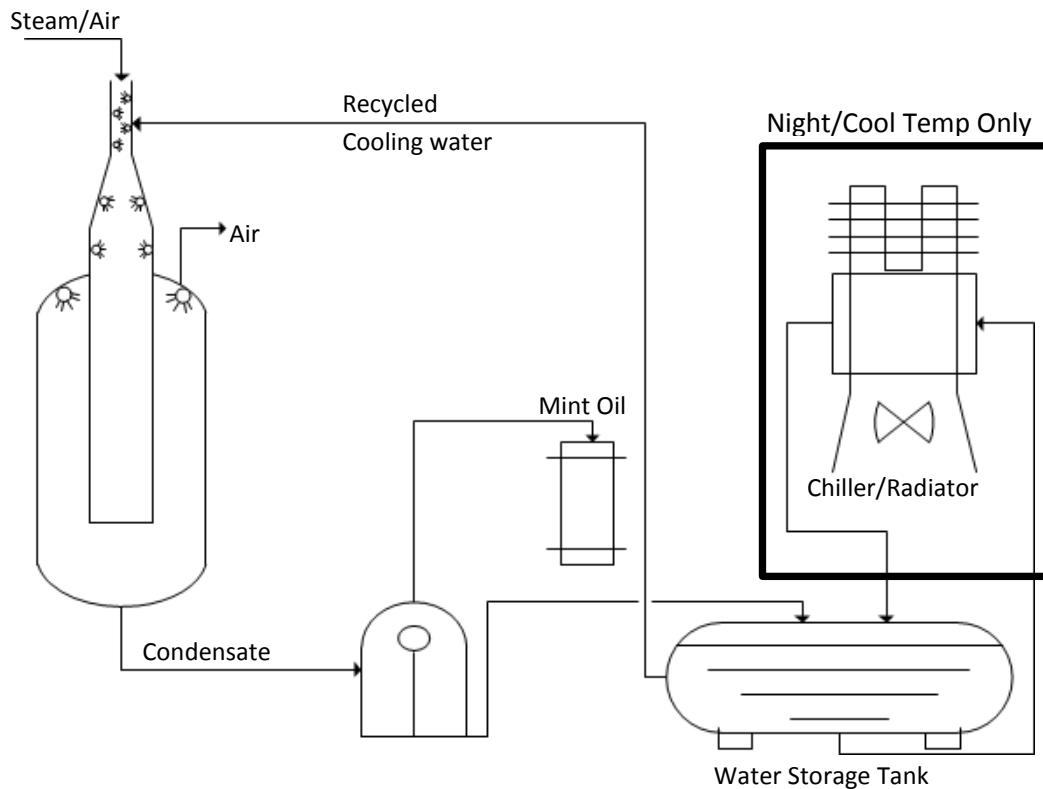


Figure 7.31- Flow diagram for coolant water recycle via large storage tank and night time forced convection air radiator for cooling.

We can estimate the size of the tank needed by the amount of cooling water based on a 100kW microwave system. Assuming the system is run for 10 hours a day and coolant water reaches just above the average nighttime low of 65°F.

$$m_{coolant} = \frac{kW}{C_p dT} = \frac{100kW}{4.2 \frac{kJ}{kg} (46^\circ C - 20^\circ C)} = 0.92 kg/s$$

$$V_{tank} = \frac{m_{coolant}}{\rho} time = \left(\frac{0.92 \frac{kg}{s}}{1000 \frac{kg}{m^3}} \right) 60 \frac{s}{min} \left(60 \frac{min}{hr} \right) 10 hrs \approx 33 m^3$$

We get approximately 33 m³ which is a very reasonable amount of space to devote to a coolant storage tank.

The second idea is to have a radiator/chiller that cools the water used during the day. This process will take up less space but will cost more in energy usage. Figure 7.32 and 7.33 show flow diagrams for these two processes. The coolant water recycle can be used with the new direct contact condenser or with the existing tube and shell condenser.

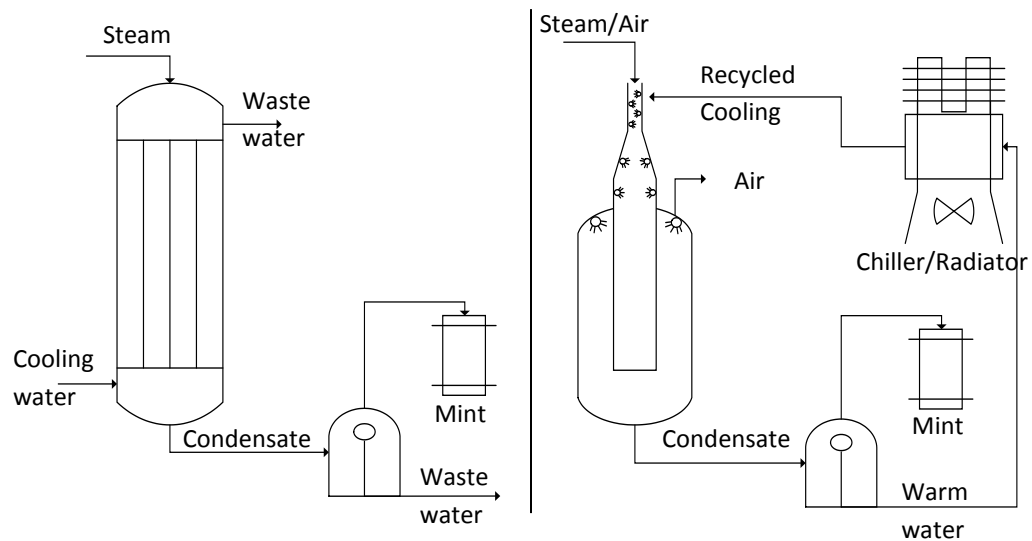


Figure 7.32 & 7.33- Flow diagram for coolant water recycle with radiator/chiller compared to the current process. The recycle process can be used with the tube and shell or the direct contact condenser.

Bibliography

- Alam, S., 2011. Peppermint Useful Herb. Pakistan & Gulf Economist.
- Al-Marzouqi, A. et al., 2007. Comparative Evaluation of SFE and Steam Distillation Methods on the Yield and Composition of Essential Oil Extracted from Spearmint (*Mentha spicata*), Journal of Liquid Chromatography & Related Technologies. Vol. 30. 463-475
- Aspen HYSYS (V 7.3) [software]. 2011. <http://www.aspentech.com/hysys/>
- Company, C. R., 1970-1971. "Handbook of Chemistry and Physics." Chemical Rubber Company handbook of chemistry and physics: 20.
- Craig, W., 2004. Peppermint's Powerful Potential. Vibrant Life. 20
- De Renzo, D.J., 1985. Corrosion Resistant Materials Handbook: Fourth Edition. Noyes Data Corporation 623,872.
- Dictionary.com, "boiler-horsepower," in Dictionary.com Unabridged. Source location: Random House, Inc. <http://dictionary.reference.com/browse/boiler-horsepower>.
- Eck, M. Zarza, E., 2006. Saturated Steam Process with Direct Steam Generating Parabolic Troughs, Solar Energy, Volume 80, Issue 11. 1424-1433
- Gershenzon, J., 2000. Regulation of Monoterpene Accumulation in Leaves of Peppermint. Plant Physiology. Vol. 122. 205-213
- Gregory S., et al., 2012. Extended Carbon Footprint Study. Mint Industry Research Council: 2011 Research Reports. 137-151.
- Hackleman, D., 2009. Solvent Free Microwave Extraction of Essential Oils Experiment Detail Report 20.
- J.G. Collier., 1935. Convective Boiling and Condensation (second Ed.)McGraw-Hill, New York
- Jenkins, J., 2012. Impact on Mint Production in the Pacific Northwest and CA of Proposed Regulatory Action to Comply with ESA. Mint Research Council: 2011 Research Reports. 51-90
- Koretsky, M., 2004. Engineering and Chemical Thermodynamics. Wiley Publishing. 192,541
- L. T. Sandborn., 1929. "l-Menthone", Org. Synth. **9**: 59; Coll. Vol. **1**: 340
- Lechler USA, Worldwide leader in spray technology. <http://www.lechlerusa.com>.

Lucchesi, M. E., F. Chemat, et al., 2004. Solvent-free microwave extraction of essential oil from aromatic herbs: comparison with conventional hydro-distillation. *Journal of Chromatography A* 1043(2): 323-327.

McConkey, M. et al., 2000. Developmental Regulation of Monoterpene Biosynthesis in the Glandular Trichomes of Peppermint. *Plant Physiology*. Vol. 122. 215-223

Pommerenck, J., et al., 2012. Recovery of a multicomponent, single phase aerosol with a difference in vapor pressure entrained in a large flow. *Journal of Chemical Thermodynamics*. 109-115

RJH ENTERPRISES, INC. Manufacturers & Distributors of the Proto Mech Incisor and Tooth Systems, Related Wood Treatment Equipment and Specialty Products. 33270 SE White Oak Road | Corvallis, Oregon 97333. <http://www.rjhenterprises.com>

Seungmin Oh, Shripad T. Revankar., 2005. Effect of noncondensable gas in a vertical tube condenser, *Nuclear Engineering and Design*, Volume 235, Issue 16, Pages 1699-1712

Seungmin Oh, Shripad T. Revankar., 2006. Experimental and theoretical investigation of film condensation with noncondensable gas, *International Journal of Heat and Mass Transfer*, Volume 49, Issues 15–16, Pages 2523-2534

Siegel-Maier, K., 1998. Peppermint: More than Just another Pretty Flavor. *Better Nutrition*. 24

Storer, F., 1864. *First Outlines of a Dictionary of Solubilities or Chemical Substances*. Cambridge: Sever and Francis. 94

Turner, G. et al., 2000. Development of Peltate Glandular Trichomes of Peppermint. *Plant Physiology*. Vol. 124. 665-679

Turner, G. et al., 2000. Distribution of Peltate Glandular Trichomes on Developing Leaves of Peppermint. *Plant Physiology*. Vol. 124. 655-663

Velasco, C., 2007. Microwave Extraction of Peppermint Oil and Comparison to the Current Practice of Steam Extraction. MS thesis, Mint Industry Research Council, Oregon State University.

Wildung, M. Croteau, R. 2005. Genetic Engineering of Peppermint for Improved Essential Oil Composition and Yield. *Transgenic Research*, 14: 365-372

APPENDICES

Appendix A. Specifications of Condenser Shell

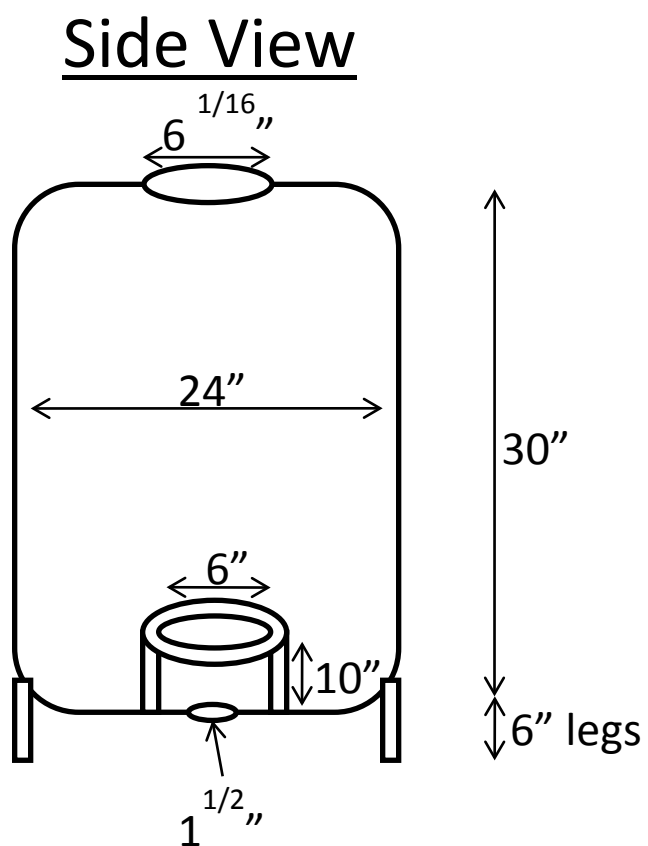


Figure A1- Side view of the direct contact condenser shell.

Appendix A. Specifications of Condenser Shell (Continued)

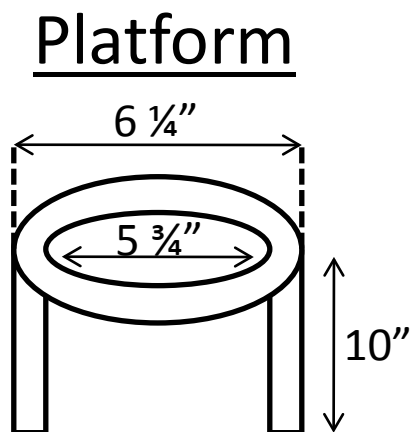


Figure A2- Center column support platform for direct contact condenser.

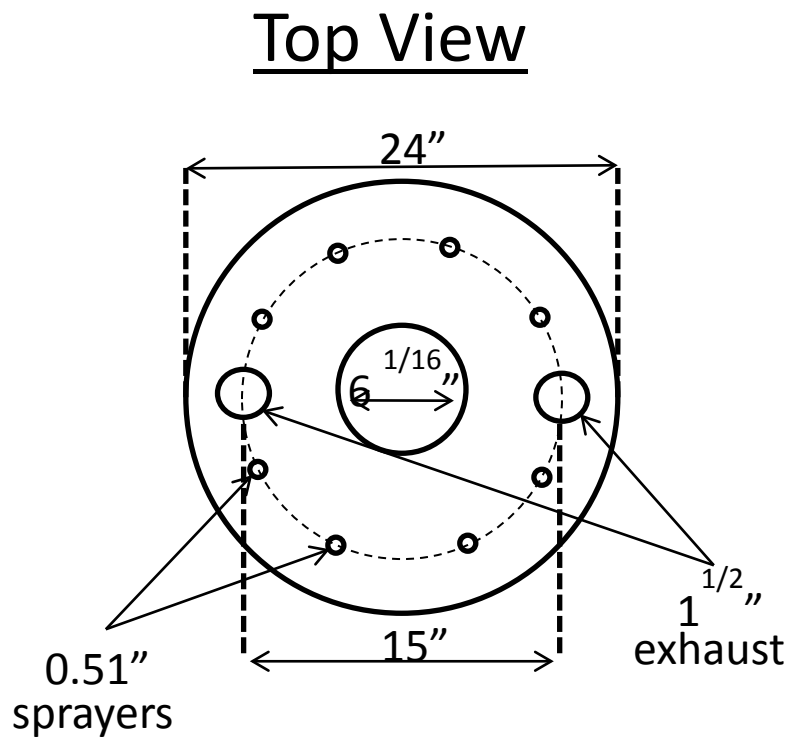


Figure A3- Top view of the direct contact condenser shell.

Appendix B. Pump Specifications

Table B1- Flotex 1.5 HP High-Capacity Thermoplastic Sprinkler Pump

Motor Voltage	NPT pipe size		Distance of Pump Above Water	GPM @ PSI							
	Inlet	Outlet		10	15	20	25	30	35	40	45
115/230	1 1/2"	1 1/2"	5'	67	66	61	55	48	39	33	18
			10'	61	58	56	52	45	37	27	14
			15'	56	55	54	51	44	34	20	8
			20'	46	45	44	43	37	28	11	0

Pump Description

The Flotec 1.5 HP High-Capacity Sprinkler Pump has a durable, fiberglass-reinforced thermoplastic housing and can handle up to 30 sprinkler heads. The pump is corrosion resistant and self primes after the housing is initially filled with water. It is great for use with automatic sprinkler systems. This pump has a high-output, dual-voltage motor and can lift water from a depth of up to 20 ft.

- Pumps up to 67 GPM or up to 45 psi
- Dual-voltage (115/230) motor provides high output
- Corrosion-resistant pump can lift water from a depth of up to 20 ft.
- Capable of handling up to 30 sprinkler heads
- Fiberglass-reinforced thermoplastic pump housing is durable
- Pump self primes after the housing is initially filled with water and is ideal for use with automatic sprinkler systems
- Fully serviceable unit for maintenance and long life
- Capable of Handling 30 Sprinkler Heads
- MFG Brand Name : Flotec
- MFG Model # : FP5172
- MFG Part # : FP5172

Pump Specifications

- **Assembled Depth (in.)** : 12 in
- **Assembled Height (in.)** : 11.75 in
- **Assembled Width (in.)** : 21.5 in
- **CSA Listed** : Yes
- **Discharge Flow @ 0 ft. (gallons/hour)** : 4020
- **Discharge Flow @ 25 ft. (gallons/hour)** : 2400
- **Discharge Pressure @ 0 ft. (psi)** : 45.0
- **Discharge Pressure @ 25 ft. (psi)** : 0.0
- **ETL Listed** : No
- **Head Pressure (ft.)** : 20.0
- **Inlet Connection** : Threaded female
- **Item Package Type** : Cardboard Container
- **Manufacturer Warranty** : 1 YEAR
- **Outlet Connection** : Threaded female
- **Portable** : No
- **Product Depth (in.)** : 12
- **Product Height (in.)** : 21.5
- **Product Weight (lb.)** : 36
- **Returnable** : 90-Day
- **UL Listed** : N-No UL Code Rating
- **Voltage (volts)** : 115/230 V



Appendix C- Nozzles Specifications (highlighted nozzle)

Material: SS316

Manufacturer: Ryan Herco Solutions (Portland)

Cost: \$35.32/nozzle



Axial full cone nozzles

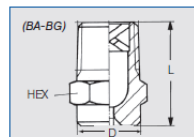
Series 460 / 461



Excellent, uniform full cone distribution and thorough atomization. X-style vane allows high free passage without heavy spots. Spray angles are consistent over the full capacity range and stable at a wide range of pressures.

Applications:

- Washing and cleaning
- Dust suppression
- Mist eliminator washing
- Chemical reactors
- Surface spraying



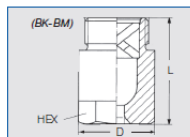
Series 460



Series 461



Plastic Version



Dimensions (in.)					
Connection Code	Inlet (Male NPT)	L	D	Hex	Weight Brass (lb.)
BA	1/8	.71	.51	9/16	.03
BC	1/4	.87	.51	9/16	.04
BE	3/8	.96/1.18*	.63	1 1/16	.07
BG	1/2	1.28/1.65*	.83	7/8	.15
BK	3/4	1.65/1.97*	1.09	1-1/8	.38
BM	1	2.20	1.32	1-3/8	.79

Subject to technical modifications

* Dimension for PVDF model

Spray angle	Ordering no.										Orifice diam. (in.)	Free passage (in.)	Flow Rate (Gallons Per Minute)											Spray Diam. D (in.) @ 30 psi	
	Type	Material no.	Connection				lines per minute											H=8"	H=20"						
			Male NPT				10	20	30	40	60	80	100	150											
			1/8"	1/4"	3/8"	1/2"	3/4"	1"	psi	psi	2 bar	psi	psi	psi	psi	psi									
90°	460.326	-	-	BA	-	-	-	-	.032	.022	.07	.09	1.4	.11	.12	.14	.16	.17	.20	15	34				
	460.406	-	-	BA	-	-	-	-	.047	.033	.17	.23	1.0	.27	.30	.35	.40	.43	15	34					
	460.446	-	-	BA	-	-	-	-	.051	.039	.22	.28	1.3	.33	.38	.44	.50	.54	15	34					
	460.486	-	-	BA	-	-	-	-	.057	.047	.28	.36	1.6	.43	.48	.57	.63	.69	15	34					
	460.526	-	-	BA	-	-	-	-	.065	.051	.35	.46	2.0	.54	.60	.71	.79	.87	15	34					
	460.566	-	-	BA	-	-	-	-	.073	.051	.43	.57	2.5	.67	.75	.88	.99	1.1	15	34					
	460.606	-	-	BA	-	BE	-	-	.081	.057	.54	.72	3.2	.84	.95	1.1	1.2	1.4	1.6	15	34				
	460.646	-	-	-	BC	BE	-	-	.091	.071	.69	.91	4.0	1.1	1.2	1.4	1.6	1.7	2.0	15	38				
	460.686	-	-	-	BC	BE	-	-	.102	.071	.86	1.1	5.0	1.3	1.5	1.8	2.0	2.2	2.5	15	38				
	460.726	-	-	-	BC	BE	-	-	.116	.079	1.1	1.4	6.3	1.7	1.9	2.2	2.5	2.7	3.2	15	38				
	460.746	-	-	-	-	BE	-	-	.130	.075	1.2	1.6	7.1	1.9	2.1	2.5	2.8	3.1	3.6	15	38				
	460.766	-	-	-	-	BE	-	-	.130	.095	1.4	1.8	8.0	2.1	2.4	2.8	3.2	3.5	4.1	15	38				
	460.806	-	-	-	-	BE	-	-	.146	.106	1.7	2.3	10.0	2.7	3.0	3.5	4.0	4.3	5.1	15	38				
	460.846	-	-	-	-	BE	-	-	.160	.126	2.2	2.8	12.5	3.3	3.8	4.4	5.0	5.4	6.4	15	38				
	460.886	-	-	-	-	BG	-	-	.185	.122	2.8	3.6	16.0	4.3	4.8	5.7	6.3	6.9	8.2	15	38				
	460.926	-	-	-	-	BG	-	-	.205	.150	3.5	4.6	20	5.4	6.0	7.1	7.9	8.7	10.2	15	38				
	460.966	-	-	-	-	BG	BK	-	.229	.150	4.3	5.7	25	6.7	7.5	8.8	9.9	10.8	12.7	15	38				
	461.006	-	-	-	-	BG	BK	-	.252	.150	5.4	7.2	32	8.4	9.5	11.1	12.5	13.7	16.1	15	38				
	461.046	-	⊗	-	-	-	BK	-	.284	.209	6.9	9.1	40	10.7	12.0	14.1	15.9	17.3	20	15	38				
	461.086	-	-	-	-	-	BK	BM	.323	.209	8.6	11.4	50	13.4	15.0	17.7	19.8	22	25	15	38				
	461.126	-	-	-	-	-	BM	-	.366	.256	10.9	14.3	63	16.9	18.9	22	25	27	32	15	38				
	461.146	-	-	-	-	-	BM	-	.390	.264	12.3	16.2	71	19.0	21	25	28	31	36	15	38				
120°	460.368	-	-	BA	-	-	-	-	.037	.028	.11	.14	.06	.17	.19	.22	.25	.27	27	48					
	460.408	-	-	BA	-	-	-	-	.047	.033	.17	.23	1.0	.27	.30	.35	.40	.43	27	48					
	460.448	-	-	BA	-	-	-	-	.051	.035	.22	.28	1.3	.33	.38	.44	.50	.54	27	48					
	460.488	-	-	BA	-	-	-	-	.059	.039	.28	.36	1.6	.43	.48	.57	.63	.69	27	48					
	460.528	-	-	BA	-	-	-	-	.065	.047	.35	.46	2.0	.54	.60	.71	.79	.87	27	48					
	460.568	-	-	BA	-	-	-	-	.075	.053	.43	.57	2.5	.67	.75	.88	.99	1.1	27	48					
	460.608	-	-	BA	-	-	-	-	.083	.055	.54	.72	3.2	.84	.95	1.1	1.2	1.4	1.6	27	48				
	460.648	-	-	-	BC	BE	-	-	.097	.063	.69	.91	4.0	1.1	1.2	1.4	1.6	1.7	2.0	27	52				
	460.688	-	-	-	BC	BE	-	-	.108	.071	.86	1.1	5.0	1.3	1.5	1.8	2.0	2.2	2.5	27	52				
	460.728	-	-	-	BC	BE	-	-	.122	.075	1.1	1.4	6.3	1.7	1.9	2.2	2.5	2.7	3.2	27	52				
	460.748	-	-	-	-	BE	-	-	.130	.075	1.2	1.6	7.1	1.9	2.1	2.5	2.8	3.1	3.6	27	52				
	460.768	-	-	-	-	BE	-	-	.138	.075	1.4	1.8	8.0	2.1	2.4	2.8	3.2	3.5	4.1	27	52				
	460.808	-	-	-	-	BE	-	-	.150	.095	1.7	2.3	10.0	2.7	3.0	3.5	4.0	4.3	5.1	27	52				
	460.848	-	-	-	-	BE	-	-	.165	.106	2.2	2.8	12.5	3.3	3.8	4.4	5.0	5.4	6.4	27	52				
	460.888	-	-	-	-	BE	BG	-	.181	.122	2.8	3.6	16.0	4.3	4.8	5.7	6.3	6.9	8.2	27	52				
	460.928	-	-	-	-	BG	-	-	.209	.130	3.5	4.6	20	5.4	6.0	7.1	7.9	8.7	10.2	27	52				
	460.968	-	-	-	-	BG	BK	-	.232	.162	4.3	5.7	25	6.7	7.5	8.8	9.9	10.8	12.7	27	52				
	461.048	-	-	-	-	-	BK	-	.299	.193	6.9	9.1	40	10.7	12.0	14.1	15.9	17.3	20	27	52				
	461.128	-	⊗	-	-	-	-	BM	.378	.260	10.9	14.3	63	16.9	18.9	22	25	27	32	27	52				
	461.148	-	-	-	-	-	BM	-	.394	.260	12.3	16.2	71	21	19.0	25	28	31	36	27	52				

Example Type + Material no. + Conn. - Ordering no.
for ordering: 460.728 + 17 + BE - 460.728.17.BE

- ⊗ Material PP (Material no. 53)
* Only available in connection BE
** Only available in connection BG
*** Only available in connection BM

The folded page on the back cover of this catalog provides a listing of alternatives of various assembly possibilities. For more information on assembly accessories, please refer to the Accessories section beginning on page 119.

Full cone

